DMD Fast Forward. Published on May 11, 2007 as doi:10.1124/dmd.107.016105

"DMD #16105"

METABOLISM, DISTRIBUTION AND EXCRETION OF A SELECTIVE NMDA RECEPTOR ANTAGONIST, TRAXOPRODIL, IN RATS AND DOGS

CHANDRA PRAKASH, DONGHUI CUI, MICHAEL J, POTCHOIBA, and TODD BUTLER

Departments of Pharmacokinetics, Dynamics and Metabolism (CP, DC, MJP) and Medicinal Chemistry (TB), Pfizer Global Research and Development, Groton, CT 06340

DMD Fast Forward. Published on May 11, 2007 as DOI: 10.1124/dmd.107.016105
This article has not been copyedited and formatted. The final version may differ from this version.

"DMD #16105"

BIOTRANSFORMATION OF A 4-PHENYLPIPERIDINE ANALOG

Address for Correspondence:

Chandra Prakash, Ph. D.
Pharmacokinetics, Dynamics and Metabolism
Pfizer Global Research and Development
Groton, CT 06340
Ph. No. 860-441-6415
Fax No. 860-686-0654
Email: Chandra.prakash@pfizer.com

Abstract	247
Introduction	497
Discussion	1357
Text pages	41
Tables	8
Figures	10
References	34

Abbreviations: NMDA, N-methyl-D-aspartate; i.v., intravenous; EM, extensive metabolizer; PM, poor metabolizer; LE, Long-Evans; WBAL, whole-body autoradioluminography; radio-HPLC, HPLC with on-line radioactivity detector; LC-MS/MS, liquid chromatography-tandem mass spectrometry; 3-hydroxy- traxoprodil, 4-[1-hydroxy-2-(4-hydroxy-4-phenyl-piperidin-1-yl)-propyl]-benzene-1,2-diol; 3-methoxy-TRX, (1S, 2S)-1-(4-hydroxy-3-methoxyphenyl)-2-(4-hydroxy-4-phenylpiperidino)-1-propanol; 4'-hydroxy-TRX, 1-[2-hydroxy-2-(4-hydroxy-phenyl)-1-methylethyl]-4-(4-hydroxy-phenyl)-piperidin-4-ol; β̃-RAM, radioactive monitor; CID, collision induced dissociation; LSC, liquid scintillation counting;; UDPGA, uridinediphosphoglucuronic acid; GIT, gastrointestinal tract; CYP450, cytochrome P450.

DMD Fast Forward. Published on May 11, 2007 as DOI: 10.1124/dmd.107.016105
This article has not been copyedited and formatted. The final version may differ from this version.

Abstract

Disposition of traxoprodil (TRX), a selective antagonist of the NMDA class of glutamate receptor, was investigated in rats and dogs after administration of a single i.v. bolus dose of [^{14}C]TRX. Total mean recoveries of the radiocarbon were 92.5 and 88.2% from rats and dogs, respectively. Excretion of radioactivity was rapid and nearly complete within 48 h after dosing in both species. Whole-body autoradioluminography study suggested that TRX radioactivity were retained more by uveal tissues, kidney and liver than by other tissues. TRX is extensively metabolized in rats and dogs since only 8-15% of the administered radioactivity was excreted as unchanged drug in the urine of these species. The metabolic pathways included aromatic hydroxylation at the phenylpiperidinol moiety, hydroxylation at the hydroxyphenyl ring and O-glucuronidation. There were notable species-related qualitative and quantitative differences in the metabolism of TRX in rats and dogs. The hydroxylation at 3-position of the phenol ring followed by methylation of the resulting catechol intermediate and subsequent conjugation were identified as the main metabolic pathways in dogs. In contrast, the major metabolites in rats were due to oxidation at 4' position of the phenylpiperidinol moiety followed by further oxidation and Phase II conjugation. TRX glucuronide conjugate was identified as the major circulating component in rats while the glucuronide and sulfate conjugates of O-methyl catechol metabolite were the major metabolites in dog plasma. The site of conjugation of regioisomeric glucuronides were established from the differences in the CID product ion spectra of their methylated products.

DMD Fast Forward. Published on May 11, 2007 as DOI: 10.1124/dmd.107.016105
This article has not been copyedited and formatted. The final version may differ from this version.

Accumulating evidence suggests that in cerebral ischaemic or hypoxic conditions such as stroke and head trauma the NMDA[1] receptor is over stimulated by an increased amount of endogenous glutamate (Bullock et al., 1992; Wood and Hawkinson, 1997; Palmer, 2001; Chazot, 2004). This event results in a massive Ca^{2+} influx into the post-synaptic neurons, activating several destructive cascades and ultimately leading to excitotoxic cell death. Glutamate receptor activity is also hypothesized to play a role in the neuron death associated with chronic neurodegenerative conditions such as Alzheimer's disease and Parkinson's disease. In these later conditions, subtle but chronic deregulation in neuronal energy metabolism renders neurons susceptible to excitotoxicity from physiological glutamate receptor activity (Maragos et al., 1987; Albin and Greenamyre, 1992; Green and Greenamyre, 1996). Therefore, selective antagonists of NMDA receptors have the potential to prevent neuronal death associated with neurodegenerative diseases and brain injury mediated by glutamate in humans.

TRX, {1-[2-hydroxy-2-(4-hydroxy-phenyl)-1-methyl-ethyl]-4-phenyl-piperidin-4-ol}mesylate, fig. 1}, is a new NMDA antagonist that is highly selective for receptors containing NR2B and are expressed in forebrain neurons (Chenard et al, 1995; Menniti et al., 1997; Chazot, 2000). It potently (IC_{50} = 11 nM) inhibits the glutamate-induced death of rat hippocampal neurons in primary cultures receptors (Menniti et al., 1997). Based on pharmacological profile *in vitro* and the *in vivo* efficacy in a number of animal models of traumatic brain injury and ischemia suggest that TRX has the potential for therapeutic effects in neurodegenerative conditions in human's ischemia (Di et al., 1997; Tsuchida et al., 1997; Menniti et al., 1998, 2000). Clinical trials in normal volunteers and head trauma patients have shown that it is well tolerated at plasma concentrations well above the efficacious concentration in animal models of brain injury and it

decreases morbidity and improves outcomes at 6 months (Menniti et al., 1998; Bullock et al., 1999; Merchant et al., 1999).

Preclinical pharmacokinetic studies in rats and dogs suggested that TRX is extensively metabolized and readily distributed into extravasicular tissue. TRX is eliminated mainly by Phase I oxidative metabolism mediated by CYP2D6 isozyme in EMs and by Phase II conjugation and renal clearance of parent in PMs (Johnson et al., 2003). Metabolic pathways of drug candidates in laboratory animals, used for safety evaluation studies, are required to ensure that the selected animal species are exposed to all major metabolites formed in humans (Baillie et. al., 2002). The objective of the present study was to characterize the disposition of TRX in rats and dogs and to identify and quantify its metabolites after a single i.v. bolus dose of [^{14}C]TRX. Metabolic profiling and identification of these metabolites were done by LC-MS/MS with radioactivity detection. Where possible, the proposed structures were supported by comparisons of their retention times on HPLC and MS spectra with those of synthetic standards. The sites of conjugation of glucuronides were established from the differences in the CID product ion spectra of their methylated products. Information generated from this study was used to support the nonclinical safety evaluation of TRX.

Materials and Methods

General Chemicals. Commercially obtained chemicals and solvents were of HPLC or analytical grade. β-Glucuronidase (from Helix Pomatia, type H-1 with sulfatase activity) was obtained from Sigma Chemical Company (St. Louis, MO). BDS hypersil C-18 HPLC analytical and preparative columns were obtained from Keystone Scientific (Bellefonte, PA). YMC basic C-18 column was purchased from YMC (Wilmington, DE). Ecolite (+) scintillation cocktail was

obtained from ICN (Irvine, CA). Carbosorb and Permafluor E+ scintillation cocktails were purchased from PerkinElmer Life and Analytical Sciences (Boston, MA). HPLC grade acetonitrile, methanol and water, and certified ACS grade ammonium acetate and acetic acid were obtained from Fisher Scientific Company (Springfield, NJ). Diazomethane was generated just before use from 1-methyl-3-nitro-1-nitrosoguanidine obtained from Sigma-Aldrich Co. (Milwaukee, WI).

Radiolabeled Drug and Reference Compounds. [^{14}C]TRX, specific activity 3.33 mCi/mol (Fig. 1), was synthesized by the Radiosynthesis Group at Pfizer Global Research and Development (Groton, CT) as described (McCarthy et. al., 1997). It showed a radiochemical purity of ≥98%, as determined by HPLC using an in-line radioactivity detector.

Synthesis of M8 [1-[2-hydroxy-2-(4'-hydroxy-phenyl)-1-methyl-ethyl]-4-(4-hydroxy-phenyl)-piperidin-4-ol]. M8 was synthesized in five steps starting from 1-(4-hydroxy-phenyl)-propan-1-one (**1**, fig. 2).

Step 1 & 2. 1-(4-Benzyloxy-phenyl)-2-bromo-propan-1-one (**5**) was prepared from 1-(4-hydroxy-phenyl)-propan-1-one (**1**) via benzylation (to give **3**) and bromination as described by Chenard et al (1991)

Step 3. A mixture of **1'(R_3=OH)** (Guzikowski et al., 2000) (0.27 g, 1.40 mmol), 1-(4-benzyloxy-phenyl)-2-bromo-propan-1-one (**5**) (0.42 g, 1.32 mmol), and triethylamine (0.40 ml, 2.87 mmol) was refluxed for 90 min. After concentration, the residue was dissolved in ethyl acetate (EtOAc), washed with water and aqueous sodium chloride and dried (over $CaSO_4$). Evaporation of the solvent gave a red foam (0.39 g), which was purified by silica gel flash chromatography, flushing first with 20% EtOAc/hexanes and then eluting with 50% EtOAc/hexanes. Solvent removal yielded **7** as a pink tinted foam (0.32 g, 56%). [FAB MS: *m/z*

432 (MH^+); NMR ($CDCl_3$) δ 8.08 (d, J = 8.9 Hz, 2H), 7.47-7.31 (m, 5H), 7.23 (d, J = 8.7 Hz, 2H), 6.98 (d, J = 8.9 Hz, 2H), 6.78 (d, J = 8.6 Hz, 2H), 5.11 (s, 2H), 4.08 (q, J = 6.8 Hz, 1H), 2.80-2.72 (m, 3H), 2.59 (br t, J = 10.6 Hz, 1H), 2.12-1.98 (m, 2H), 1.70 (br d, J = 11.9 Hz, 2H), 1.29 (d, J = 6.7 Hz, 3H).

Step 4. A solution of **7** (0.29 g, 0.67 mmol) in ethanol (EtOH; 9 ml) was added to $NaBH_4$ dissolved in 1 ml EtOH. After stirring for 20 h, water was added and the mixture was concentrated *in vacuo* at 40-50 °C. The residue was partitioned between EtOAc and water; the organic phase was washed with aqueous sodium chloride, dried (over $MgSO_4$) and concentrated to an off-white solid (0.30 g). Flash chromatography with 50% and 75% EtOAc/hexanes yielded **9** as a white solid (0.14 g, 47%), [mp 208-212 °C; NMR ($CDCl_3$) δ 9.21 (br s, 1H), 7.47-7.24 (m, 9H), 6.96 (d, J = 8.6 Hz, 2H), 5.09 (s, 2H), 5.03 (br s, 1H), 4.62 (s, 1H), 4.22 (d, J = 9.4 Hz, 1H), 2.95 (m, 1H), 2.65-2.40 (m, 4H), 2.13-1.85 (m, 2H), 1.61 (br d, J = 12.4 Hz, 2H), 0.69 (d, J = 6.5 Hz, 3H).

Step 5. A mixture of **9** (0.112g, 0.258 mmol) and 10% $Pd(OH)_2$ on carbon (0.015 g) in methanol (MeOH) was hydrogenated (50 psi) for 22 h. Filtration (Celite) and concentration gave an oily solid which was recrystallized from EtOH/EtOAc/Et_2O to yield **M8** (**10**, racemic mixture) as a light tan solid (0.074g, 53%), [mp 180.5-181.5°C; NMR ($CDCl_3$) δ 9.22 (br s, 2H), 7.30 (d, J= 7.5 Hz, 2H), 7.13 (d, J = 7.2 Hz, 2H), 6.70 (d, J = 4.8 hz, 4H), 4.66 (s, 1H), 4.18 (d, J = 7.2 Hz, 1H), 3.10-2.95 (m, 1H), 2.70-2.35 (m, 5H), 2.17-1.75 (m, 2H), 1.62 (br d, J = 11.2 Hz, 2H), 0.69 (m, 3H);..

DMD Fast Forward. Published on May 11, 2007 as DOI: 10.1124/dmd.107.016105
This article has not been copyedited and formatted. The final version may differ from this version.

Synthesis of M12 {4-[1-hydroxy-2-(4-hydroxy-4-phenyl-piperidin-1-yl)-propyl]-benzene-1,2-diol]}. M12 was synthesized in five steps starting from 1-(3,4-dihydroxy-phenyl)-propan-1-one (**2,** fig. 2)

1-(2,2-Diphenyl-benzo[1,3]dioxol-5-yl)-propan-1-one (4) A mixture of dichlorodiphenylmethane (10.0 ml, 52.1 mmol) and **2** (5.0 g, 30.1 mmol) was heated at 170°C for 7 min, during which time rapid evolution of HCl gas was observed. The reaction was cooled, poured into 1 N NaOH and extracted into ethyl ether (Et_2O; 2x75 ml). The extracts were washed with water and aqueous sodium chloride, dried (over $MgSO_4$) and concentrated onto silica gel. Flash chromatography using a 2-10% Et_2O/hexanes gradient gave **4** as an orange oil which solidified upon standing (4.82g, 48%) [mp 69-70.5°C; NMR ($CDCl_3$) δ7.60-7.30 (m, 6H), 7.50-7.30 (m, 6H), 6.92 (d, J = 8.2 Hz, 1H), 2.92 (q, J = 7.2 Hz, 2H), 1.21 (t, J = 7.2 Hz, 3H); Anal. Calculated for $C_{22}H_{18}O_3$: C, 79.98; H, 5.49. Found: C, 80.05; H, 5.34.].

4 was converted to **M12** in 4 steps using methodology similar to that described above in the preparation of **M8.**

M12. (**12**, Racemate): mp 167-168°C (EtOH); NMR (DMSO-d_6) δ 7.53 (d, J = 7.7 Hz, 2H), 7.32 (t, J = 7.5 Hz, 2H), 7.20 (t, J = 7.0 Hz, 1H), 6.75 (s, 1H), 6.67 (d, J = 8.0 Hz, 1H), 6.58 (d, J = 8.0 Hz, 1H), 4.82 (br s, 1H), 4.09 (d, J = 9.4 Hz, 1H), 2.98 (br t, J = 10.7 Hz, 1H), 2.61-2.46 (m, 4H), 2.15-1.90 (m, 2H), 1.63 (br d, J = 12.6 Hz, 2H), 0.70 (d, J = 6.5 Hz, 3H).

Animals, Dosing and Sample Collection. Bile-duct and/or jugular vein cannulated rats (190-270 g) were purchased from Charles River Laboratories (Stoneridge, NY). Beagle dogs (9.2-10.9 kg) were from in house colony. Animals were quarantined for a minimum of 3 days prior

to treatment and maintained on a 12-h light/dark cycle. The animals were housed individually in stainless steel metabolism cages. The animals were fasted overnight prior to administration of the dose and were fed 6 h after the dose. The animals were provided water *ad libitium*. All studies were conducted in a research facility accredited by the American Association for the Accreditation of Laboratory Animal Care.

Rats. A group of jugular-vein cannulated rats (n=3/gender) was administered a single 15 mg (free base)/kg i.v. dose of [^{14}C]TRX for mass balance study. The dose was administered over approximately 1 min. To assure complete administration of the dose the line was rinsed with approximately 1 ml of sterile saline. For biliary excretion experiments, another group of two male and two female jugular-vein and bile-duct cannulated rats was administered a single 15-mg/kg i.v. dose of [^{14}C]TRX as described above. The dose was prepared by dissolving the radiolabelled TRX in 0.9% sterile saline solution at a concentration of 1.68 mg/ml. Each rat received an approximate dose of 36 to 53 μCi of radiolabelled material. Urine and feces were collected from intact animals for seven days at 0-8, 8-24, 24-48, 48-72, 72-96, 96-120, 120-144, and 144-168 h after the dose. The first feces sample was collected at 0-24 h after the dose. Bile and urine samples were collected from bile-duct cannulated animals at 0-4 and 4-8 h after the dose. The volumes of urine and bile samples were recorded and all of the biological samples were stored at -20 ^{o}C until analysis.

For pharmacokinetic experiments, a third group of jugular-vein cannulated rats (N=3/gender) were i.v. dosed a 15 mg/kg of [^{14}C]TRX. Blood (~400 μl) was collected in heparinized tubes at 0, 0.166, 0.33, 0.5, 1, 2, 4, 8, 12, and 24 h after the dose. A fourth group of animals (n=3/sex) was dosed for the identification of circulating metabolites. Blood was collected in heparinized tubes by decapitation of three male and three females at 1 and 4 h post dose. Blood samples were centrifuged at 1000 g for 10 min to obtain the plasma. Plasma was transferred to clean tubes and stored at -20 ^{o}C until analysis.

DMD Fast Forward. Published on May 11, 2007 as DOI: 10.1124/dmd.107.016105
This article has not been copyedited and formatted. The final version may differ from this version.

For whole-body autoradioluminography experiments, a fifth group of jugular-vein cannulated LE rats (N=5/gender) received 15 mg/kg (79±3.4 μCi/kg) i.v. dose of [^{14}C]TRX. Rats were euthanatized by CO_2 asphyxiation in gender pairs at 0.33, 3, 8, 24 and 168 h post-dose and prepared for whole-body autoradioluminography by immersion into a freezing chamber (-75 ^{o}C) containing dry ice and hexanes for 10 min.

Dog Study. Two male and two female beagle dogs (9.2-10.9 kg) were administered intravenously a single 5 mg/kg base equivalent dose of [^{14}C]TRX. Urine and feces were quantitatively collected from animals for 5 days at 0-6, 6-24, 24-48, 48-72, 72-96, and 96-120 h post dose. The first feces sample was collected at the 0-24 h post-dose. Another group of one male and one female dog was cannulated at the bile duct and dosed with a 5 mg/kg base equivalent dose of [^{14}C]TRX. Blood (~6 ml/time point) was collected from the jugular vein of each animal at 0, 0.25, 0.5, 1, 2, 4, 6, 8, 12, and 24 h post dose. Blood samples were collected in heparinized tubes and were spun in a centrifuge. Plasma were transferred into new tubes and stored at -20 ^{o}C until analysis. Bile was collected for at 0-4 and 4-8 post-dose. The dose was prepared by dissolving [^{14}C]TRX in 5% dextrose at a concentration of 36.1 mg/ml and each animal received about 2 ml of the dosing solution.

Determination of Radioactivity. The radioactivity in urine, bile, and plasma was determined by LSC. Aliquots of plasma, urine and bile (20-200 μl) in triplicate, for each sampling time point, were mixed with 5 ml of Ecolite (+) scintillation cocktail (ICN; Irvin, CA) and counted in a liquid scintillation counter. Fecal samples were placed in Falcon tubes (50 ml) and homogenized in water to a thick slurry using a Brinkman Polytron lab homogenizer (Brinkman; Westbury, NY). Aliquots (100-200 mg) of the fecal homogenates were air dried over night and

combusted using a Model OX-500 oxidizer (R.J. Harvey Instruments; Hillsdale, NJ). The radioactivity in combustion products was determined by trapping the liberated CO_2 in Harvey Carbon-14 scintillation cocktail, followed by LSC. Combustion efficiency was determined by combustion of ^{14}C-standard in an identical manner.

The samples obtained prior to dosing were also counted to obtain background count rate. The amount of radioactivity in the dose was expressed as 100% and the radioactivity in urine and feces at each sampling time was expressed as the percentage of dose excreted in the respective matrices at that sampling time. The amount of radioactivity in plasma was expressed as ng equivalent of parent drug per milliliter and was calculated by using the specific activity of the administered dose.

Pharmacokinetic Analysis. Plasma concentrations of the unchanged TRX were determined at Phoenix life Sciences (Saint-Laurent, Quebec Canada) by a validated HPLC/MS/MS assay. Pharmacokinetic parameters were calculated by non-compartmental analysis using WinNonlin-Pro Ver.3.2 (Pharsight; Mountain View, CA).

Whole-Body Autoradioluminography. The whole-body cryosectioning technique developed by Ullberg (1977) was used to acquire whole-body cryosections for autoradioluminography. The Micro Computer Imaging Device (Imaging Research Inc., St. Catharines, Ontario, Canada) was used to quantify the concentration of carbon-14 radioactivity in calibration curve standards, cryosection quality control samples, and tissues of whole-body cryosections (Potchoiba et al., 1995, 1998).

Extraction of Metabolites from Biological Samples. A significant portion of the radioactivity (90% of the total radioactivity) was excreted in urine during the first 48 h post-dose. Therefore,

DMD Fast Forward. Published on May 11, 2007 as DOI: 10.1124/dmd.107.016105
This article has not been copyedited and formatted. The final version may differ from this version.

urine samples collected at 0-8, 8-24 and 24-48 h post-dose were pooled on the basis of weight and the pooled samples were used for profiling and identification of metabolites. Pooled urine (~3 ml, pool) from each animal was centrifuged and the supernatant was transferred to a clean tube and concentrated under nitrogen in a Turbo Vap LV evaporator (Caliper life sciences, Hopkinton, MA). The residue was dissolved in ~1 ml of NH_4OAc buffer (pH 5.0, 20 mM)/acetonitrile (50:50) and an aliquot (50-100 µl) was injected onto the HPLC column without further purification.

An aliquot of bile (0-8 h) was diluted with 4 volumes of acetonitrile and the precipitated material was removed by centrifugation. The pellet was washed with an additional one volume of acetonitrile and both supernatants were combined. The extraction recovery of the radioactivity in bile was about 70-85% for rat bile and ~85% for dog bile. The supernatant was evaporated to dryness under nitrogen in a Turbo Vap LV evaporator and the residue was re-dissolved in NH_4OAc buffer (pH 5.0, 20 mM). The sample was applied to a preconditioned C-18 Sep-Pak (Supelco, Bellefonte, PA). The column was washed with water (3 ml) and the metabolites were eluted with methanol (3 ml). The methanol solution was evaporated to dryness under nitrogen in a Turbo Vap LV evaporator and the residue was dissolved in 600 µl of 10 mM ammonium acetate, pH 5.0/methanol (50:50). An aliquot was injected onto the HPLC column.

Fecal homogenates from 0-24 and 24-48 h were pooled on the basis of sample weight. The pooled fecal homogenates (~2 g) were diluted with methanol (6 ml). The suspension was stirred for 2 h on a magnetic stirrer, and centrifuged at 1500 g for 10 min. After supernatant transfer to clean 15-ml conical tubes, the residues were further extracted three times with 6 ml of methanol as described above. The overall recovery of radioactivity in feces was about 78-85% after

extraction for both species. The methanol extracts were combined and concentrated under nitrogen in a Turbo Vap LV evaporator. The residues were reconstituted in 1 ml of HPLC mobile phase and aliquots (50-100 µl) were injected onto the HPLC column without further sample purification.

For rats, plasma (3 ml pooled, at 1 and 4 h post dose) was diluted with 9 ml of acetonitrile and the precipitated protein was removed by centrifugation. The pellets were extracted with an additional 2 ml of acetonitrile. The extraction recovery of the radioactivity in plasma was about 80-88%. The supernatants from the two extractions were combined and concentrated under nitrogen in a Turbo Vap LV evaporator. The residues were reconstituted in 500 µl of HPLC mobile phase and aliquots (100 µl) were injected onto the HPLC column without further sample purification.

For dogs, plasma (9 ml, 0-24 h pool, 1 ml from each time point) was diluted with 4 volumes of acetonitrile and the precipitated protein was removed by centrifugation. The pellet was washed with an additional 5 ml of acetonitrile and the supernatants from the two washes were combined. The extraction recovery of the radioactivity in plasma was about 78-85%. The supernatant was concentrated on a Speed Vac, and the residue was reconstituted in 400 µl of methanol:20 mM ammonium acetate (1:1). An aliquot (80 µl) was injected on the LC/MS.

HPLC. HPLC system consisted of an HP-1100 solvent delivery system, an HP-1100 membrane-degasser, an HP-1100 autoinjector (Hewlett Packard, Palo Alto, CA), and a radioactivity monitor (ß-RAM, IN/US, Tampa, FL). Chromatography was performed on a BDS Hypersil C-18 column (4.6 mm x 250 mm, 5 µm) with a mobile phase containing a mixture of

DMD Fast Forward. Published on May 11, 2007 as DOI: 10.1124/dmd.107.016105
This article has not been copyedited and formatted. The final version may differ from this version.

10 mM ammonium acetate, pH 5.0 (solvent A) and acetonitrile (solvent B). The mobile phase was initially composed of solvent A/solvent B (95:5), and held for 5 min. The mobile phase composition was then linearly programmed to solvent A/solvent B (75:25), over 20 min. A short gradient was programmed to solvent A/solvent B (10:90) over 5 min, and these conditions were held for 7 min. The mobile phase composition was returned to the starting solvent mixture over 3 min. The system was allowed to equilibrate for approximately 15 min before making the next injection.

For bile samples, chromatography was performed on a YMC basic C-18 column (4.6 mm x 250 mm, 5 μm) with a mobile phase containing a mixture of 10 mM ammonium acetate, pH 5.0 (solvent A) and methanol (solvent B). The mobile phase was initially composed of solvent A/solvent B (95:5), and held for 5 min. The mobile phase composition was then linearly programmed to solvent A/solvent B (70:30), over 25 min, and these conditions were held for 2 min. A short gradient was and programmed to solvent A/solvent B (40:60) over 7 min, and these conditions were held for 7 min. The mobile phase composition was returned to the starting solvent mixture over 5 min. The system was allowed to equilibrate for approximately 15 min before making the next injection. A flow rate of 1.0 ml/min was used for all analyses. The HPLC column recoveries were 95-99% for all matrices.

Quantitative Assessment of Metabolites. Quantification of the metabolites was carried out by measuring radioactivity in the individual HPLC-separated peaks using a β-RAM. The β-RAM provided an integrated printout in counts per minute and percentage of the radiolabelled material, as well as peak representation. The β-RAM was operated in the homogeneous liquid

scintillation counting mode, with addition of 3 ml/min of Tru-Count scintillation cocktail to the effluent after UV detection.

The radiochromatograms of metabolites in rat plasma were generated by collecting fractions at 0.5 min intervals and counting the fractions in a liquid scintillation counter. The retention times of the radioactive peaks, where possible, were compared with those of synthetic standards and characterization of the major metabolites was carried out by LC-MS/MS.

LC-MS/MS: LC-MS/MS was conducted with a PerkinElmer-Sciex API III^+ spectrometer (Toronto, Canada). The effluent from the HPLC column was split and about 50 µl/min was introduced into the atmospheric ionization source via a pneumatically assisted electrospray interface. The remaining effluent was directed into the flow cell of the β-RAM. The β-RAM response was recorded in real time by the mass spectrometer that provided simultaneous detection of radioactivity and mass spectrometry data. The delay in response between the two detectors was about 0.2 min with the mass spectrometric response recorded earlier. The ionspray interface was operated at 5000 V and the mass spectrometer was operated in the positive ion mode. CID studies were performed using argon gas at the collision energy of 24 eV and a collision gas thickness of 2.6×10^{14} molecules/cm^2.

Enzymatic *in Vitro* Synthesis of the Glucuronides. Phenobarbital induced rat liver microsomes (RLPB-2) were used for the generation of glucuronide conjugates of TRX and 4'-hydroxy-TRX. Microsomal incubation mixture, in a final volume of 1 ml, contained 100 mM potassium phosphate buffer (pH 7.4), 1 mM substrate, microsomes (3 mg protein/ml incubation mixture), 10 mM $MgCl_2$, triton X-100 (0.05%) and 10 mM UDPGA. The mixture was incubated

at 37°C for 2 h and terminated by adding 2 ml of methanol. The solution was vortexed, centrifuged at 1800 g for 10 min. The supernatant was evaporated to dryness; the residue was reconstituted in HPLC mobile phase and analyzed by HPLC.

Enzymatic Hydrolysis. Pooled rat bile and urine samples (0.5 ml each) were adjusted to pH 5 with sodium acetate buffer (0.1 M) and treated with 2,500 units of β-glucuronidase/sulfatase (Prakash and Soliman, 1997). The mixture was incubated in a shaking water bath at 37 °C for 12 h and was diluted with acetonitrile. The precipitated protein was removed by centrifugation. The pellet was washed with an additional 2 ml of acetonitrile and the two supernatants were combined. The supernatant was concentrated and dissolved in 0.5 ml of mobile phase, and an aliquot (50 µl) was injected into the HPLC system. Incubation of bile and urine samples for 12 h without the enzyme served as a control.

Derivatization. The glucuronide conjugates of 4'-hydroxy-TRX were separated, isolated by HPLC and methylated with diazomethane as previously described (Johnson et al., 2003). The compound (100 - 200 ng) was dissolved in methanol (100 µl) and freshly prepared ethereal diazomethane (200 µl) was added. After standing for 30 min at room temperature the solvent was removed by a stream of nitrogen and the residue was dissolved in the HPLC mobile phase.

Results

^{14}C-Excretion. *Rats*. After iv administration of a single 15 mg/kg dose of [^{14}C]TRX to LE rats, a major portion of the radioactivity was recovered in the feces in male rats and urine and feces of female rats (Table 1A). The male rats excreted 19.5 and 50.1% of the radioactive dose in urine and feces, respectively, during the initial 0-24 h, and 21.6 and 70.5% over 168 h. On the other hand, the female rats excreted 31.5 and 25.3% of the dose in urine and feces, respectively, during the 0-24 h and 41.0 and 51.7% over 168 h. In total, 92.1 of the radioactive dose was

recovered from male rats and 92.7% from female rats (Table 1A). Essentially entire administered dose was recovered within 48 h.

Dogs. A total of 82.4 and 94.1% the administered radioactive dose was recovered in urine and feces of male and female beagle dogs, respectively (Table 1B). The male dogs excreted 29.7 and 52.7% of the radioactive dose in urine and feces, respectively, during the 0-120 h post dose (Table 1). The female dogs excreted 48.2 and 45.9% of the dose in urine and feces, respectively, during the 5 day period. Of the entire radioactivity recovered in the urine and feces, >95%, was excreted in the first 48 h after dose administration.

Pharmacokinetics. *Rats*. Mean plasma concentration versus time curves of TRX and total radioactivity after a single 15 mg/kg i.v. dose of [^{14}C]TRX to rats are shown in Fig. 3. The mean plasma concentrations of TRX (at first time point) were 416 and 683 ng/ml for male and female rats, respectively (Table 2). The mean peak plasma concentrations for total radioactivity were 1470 and 1750 ng eq/ml for male and female rats, respectively (Table 2). Mean AUC(0-∞) values for unchanged TRX were 388 and 626 ng.h/ml, respectively, in male and female rats. Mean $AUC_{(0-12)}$ values for total radioactivity were 3440 and 3730 ng-eq.h/ml in male and female rats, respectively. The elimination of TRX in both male and female rats was relatively rapid with a mean $T_{1/2}$ of 1.5 h. The elimination of radioactivity was slower compared to parent drug with a mean $T_{1/2}$ of 8.6 h.

Dogs. Mean plasma concentration versus time curves of TRX and total radioactivity after a single 5 mg/kg i.v. dose of [^{14}C]TRX to dogs are shown in Fig. 4. The mean plasma concentration of TRX at first time point (0.25 h) post dose was 418 ng/ml for male dogs, and 585 ng/ml for female dogs. The mean plasma concentrations for total radioactivity at first time

point (0.25 h) post dose were 1570 and 1750 ng.eq/ml for male and female dogs, respectively (Table 2). Mean AUC(0-∞) values for unchanged TRX were 1620 and 2550 ng.h/ml, respectively, in male and female dogs. Mean $AUC_{(0-24)}$ values for total radioactivity were 26000 and 32200 ng-eq.h/ml in male and female dogs, respectively. The elimination of TRX in both male and female dogs was rapid with a mean $T_{1/2}$ of 5.0 h. The elimination of radioactivity was slower compare to parent drug with a mean $T_{1/2}$ of 40.7 h. Based on $AUC_{(0-24)}$ values, only <7% of the circulating radioactivity was attributable to the unchanged drug for both male and female dogs.

Tissue Distribution. The concentrations of radioactivity in tissues after i.v. administration of [^{14}C]TRX to rats are shown in Table 3. Drug-related radioactivity distributed rapidly to most tissues and organs of LE rats, with maximum concentrations achieved at 0.33 or 1 h. All tissues contained higher concentrations of drug radioequivalents than that observed for blood except for the testis in the male rat. The greatest amounts of radioactivity were present in the GIT contents over the time course of 0.33 to 8 h in the female rat and at 0.33 and 3 h in the male rat. This presence of radioactivity in GIT contents resulted from the elimination of drug radioactivity in bile. Excluding drug radioactivity in the GIT contents, the uvea, a melanin containing structure of the eye, contained the greatest amount of [^{14}C]radioactivity over the time course of this study regardless of gender. Drug radioactivity was of similar concentrations in most tissues of the female rat compared to those corresponding tissues of the male rat except for possibly the salivary gland where drug radioactivity was 1.7-fold higher for the female rat. Drug radioactivity did distribute into the brain of both rat genders by 0.33 h at concentrations that were 1.7 and 1.5-fold higher than blood concentrations for the female and male rat, respectively. Since radioactivity in brain and blood was not detected by 3 h, there was apparently rapid

elimination of the parent drug, and any drug-related metabolites. By 8 h drug radioactivity was still present in the lacrimal gland, kidney, liver, salivary gland, and uvea. Drug radioactivity was sustained in only the liver, kidney, and uvea for 24 h post dose of both rat genders. This persistence of radioactivity in the liver and kidney clearly suggested that [^{14}C]TRX radioactivity was removed from the body by both hepatic and renal elimination. The mean elimination $t_{1/2}$ of [^{14}C]TRX radioactivity from female and male rat livers and kidneys were estimated to be 9 and 6.5 h, respectively. By 168 h, drug radioactivity was present only in the uvea of both rat genders indicating an affinity for melanin (data not shown). A slow elimination of radioactivity was observed from the uvea with a mean elimination $T_{1/2}$ of 80 h.

Metabolic profiles

Rat Urine. A representative metabolic profile in urine from rats following i.v. administration of [^{14}C]TRX is shown in Fig. 5. There were no qualitative differences in the urinary metabolic profiles between male and female rats. The metabolites were quantified with on line integration of the radio-chromatographic peaks. The percentages of urinary metabolites excreted in relation to the administered dose are presented in Table 4. Unchanged parent and a total of thirteen metabolites were identified in urine. The major urinary metabolites were M6 (7.5%) and M8 (6.20%). The identified metabolites and TRX accounted for >90% of the total radioactivity present in urine.

Rat Feces. A representative HPLC-radio chromatogram of fecal metabolites from rats is shown in Fig. 5. The mean percentage of fecal metabolites in relation to total radioactivity extracted from the feces for male and female rats is presented in Table 4. Most of the radioactivity in

feces was due to metabolites and little parent drug (<2% of the dose) was detected. The major fecal metabolites were M5 (26.5%), M8 (16.2 %), M10 (4.01%) and M12 (1.35%).

Rat Bile. Bile samples (0-8 h) from one male and one female rat were used for profiling and identification of metabolites. The bile sample was extracted and purified as described in the method section. The extraction recovery of the radioactivity in bile was about 70-80%. A representative HPLC-radiochromatogram of biliary metabolites from one male and one female rat are shown in Fig 6. The percentage of bile metabolites in relation to total radioactivity excreted in bile is presented in Table 5. TRX and a total of twelve metabolites (85% of the recovered radioactivity) were identified in bile. The major biliary metabolites included M1 (5.22%), M2 (8.90%), M3 (11.0%), M6 (18.1%), M7 (8.96%), M8 (15.1%), M9 (2.49%) and M10 (5.47%).

Rat Circulating Metabolites. A representative reconstructed HPLC-radio chromatogram of plasma metabolites (1 and 4 h time points pooled) is given in Fig. 6. The percentage of metabolites in relation to the total radioactivity extracted from the plasma of both male and female rats is presented in Table 6. There was no qualitative difference in the metabolic profiles between male and female rats. The amount of unchanged TRX was about the same in both male and female rats. In addition to parent drug, a total of seven metabolites were identified in plasma. The major circulating metabolite was M6 (35.5%). The identified metabolites and unchanged drug accounted for approximately 86% of the total radioactivity present in plasma.

Dog Urine. A representative metabolic profile of urinary metabolites in dogs following i.v. administration of [^{14}C]TRX is shown in Fig. 7. A total of 6 metabolites were identified in dog

urine. The percentages of metabolites excreted in urine of male and female dogs are presented in Table 7. There were no qualitative differences in the urinary metabolic profiles between male and female dogs. The major urinary metabolites were M7 (1.8%) and M14 (13.9%). The identified metabolites including unchanged drug accounted for 85% of the total radioactivity present in urine (approximately 32% of the dose). The remaining radioactive components were present only in very small amounts and could not be characterized.

Dog Feces. A major portion of the radioactivity (about 95% of the total radioactivity in feces) was excreted in feces during the first 48 h after iv administration of TRX. Therefore, fecal homogenates from 0-24, 24-48 h were pooled on the basis of sample weight for profiling and identification of metabolites. The pooled fecal homogenates were extracted and purified as described in the method section. The overall recovery of radioactivity in feces was about 78-85% after extraction. A representative HPLC-radiochromatogram of fecal metabolites in dogs is given in Fig 7. The percentages of fecal metabolites in male and female dogs are presented in Table 7. Three metabolites (M12, 8.0%; M13, 22.8%; M11, 2.0%) and the unchanged drug (13%) accounted for approximately 91% of the total radioactivity (45% of the dose) in feces.

Dog Bile. Bile samples (0-8 h) from one male and one female dog were used for profiling and identification of metabolites. The pooled bile sample was extracted and purified as described in the method section. The extraction recovery of the radioactivity in bile was about 85%. The HPLC-radiochromatogram of biliary metabolites in dogs is shown in Fig.8. The percentages of bile metabolites in relation to total radioactivity excreted from bile are presented in Table 5. In addition to TRX, 6 metabolites (89% of the total radioactivity) were identified in bile. All these

metabolites were also detected in urine. There were no qualitative differences of biliary metabolites between male and female dog.

Circulating Metabolites. Plasma (0-24 h) samples from each animal (1.0 ml, from each time point) were pooled by sex and deproteinized with acetonitrile. Plasma from male and female dogs were profiled and analyzed by mass spectrometry. The HPLC-radio chromatogram of the plasma metabolites (0-24 h) from one dog is given in Fig. 8. The percentage of the metabolites in relation to the total radioactivity extracted from the plasma of both male and female dogs is presented in Table 6. The amount of unchanged TRX and 3-methoxy-TRX accounted for 73% and 78% in the male and female dog plasma, respectively. Unchanged drug and a total of 4 metabolites accounted for approximately 84% of the total radioactivity present in plasma.

Identification of Metabolites. The structures of metabolites were elucidated by ion spray LC/MS/MS using combination of full and product ion scanning techniques (Kamel and Prakash, 2006; Prakash et al., 2007). The structures of major metabolites, where possible, were supported by comparisons of their retention times on HPLC and MS spectra with those of synthetic standards.

Glucuronide Conjugates from Microsomal Incubations

The HPLC/UV chromatogram of the incubation mixture of 4'-hydroxy-TRX with PB induced rat liver microsomes showed two additional peaks (not shown). Full-scan MS of both peaks displayed the same protonated molecular ion at *m/z* 520, 176 Da higher than the parent drug, suggesting the presence of two glucuronide regioisomers. The CID product ion spectra of both

regioisomers were identical and gave the intense ions at *m/z* 326, 176, 151 and 147 (Fig. 9a and 10a).

Treatment of first peak with diazomethane gave a product that showed a protonated molecular ion at *m/z* 548, 28 Da higher than the parent compound, indicative of the addition of two methyl groups. The CID product ion spectrum of *m/z* 548 (methylated product) showed the fragment ions at *m/z* 530 $(MH\text{-}H_2O)^+$, 512 $((MH\text{-}H_2O\text{-}H_2O)^+$, 340 $(MH\text{-}H_2O$-methyl glucuronide$)^+$, 190, 161 and 151 (Fig. 9b). The fragment ions at m/z 530 and 512 suggested that both alcoholic hydroxyl groups were unsubstituted. The fragment ions at *m/z* 190 and 161, 14 Da higher than the fragment ions to those observed in the CID spectrum of glucuronide, suggested that the methylation had occurred at the phenolic hydroxyl group of the phenyl-piperidine ring. The other prominent fragment ion at *m/z* 151 suggested that the glucuronidation had occurred at the phenolic group of the phenyl-ethyl portion of the molecule.

Treatment of second peak with diazomethane gave a product that showed a protonated molecular ion at *m/z* 548, 28 Da higher than the parent compound, indicative of the addition of two methyl groups. The CID product ion spectrum of its methylated product showed the fragment ions at *m/z* 530 $(MH\text{-}H_2O)^+$, 512 $((MH\text{-}H_2O\text{-}H_2O)^+$, 340 $(MH\text{-}H_2O$-methyl glucuronide$)^+$, 176, 165 and 147 (Fig 6b). The fragment ions *at m/z* 530 and 512 suggested that the both alcoholic hydroxyl groups were unsubstituted. The fragment ions at *m/z* 176 and 147 were similar to those observed in the CID spectrum of glucuronide, suggested that the phenolic group of the phenyl-piperidine ring was substituted. The prominent fragment ions at m/z 366, 165 further suggested that the glucuronidation had occurred at the phenolic group of the phenyl-piperidine ring.

Based on these data, it was determined that glucuronidation of 4'-hydroxy-TRX occurred primarily on the phenolic hydroxyl groups of the molecule rather than on the alcoholic hydroxyl groups.

Metabolites M1 and M3. Metabolite M1 was present only in rat urine while M3 was observed in rat urine, bile and plasma. Both M1 and M3 showed a protonated molecular ion at *m/z* 520, 192 (176+16), Da higher than the parent drug suggesting that they were glucuronide conjugates of a hydroxy metabolite. M1 and M3 had the similar retention times and identical CID mass spectra as the glucuronide conjugates obtained from *in vitro* incubations of 4'-hydroxy-TRX (Table 8). Based on these data, M1 was identified as the glucuronide of 4'-hydroxy-TRX with the glucuronic acid moiety on the hydroxyl group attached to the phenylethyl portion of the molecule and M3 was identified as the glucuronide of 4'-hydroxy-TRX with the glucuronic acid moiety on the phenolic hydroxyl group of the phenyl group attached to piperidine ring.

Metabolites M2. M2 had a retention time of 15.0-15.5 min on HPLC and was detected in rat urine and bile. M2 showed a protonated molecular ion at *m/z* 550, 222 Da higher than the parent molecule, suggesting that it was a conjugate. The CID product ion spectrum of *m/z* 550 gave prominent and significant ions at *m/z* 532, 514, 374, 356, 181, 176, 163 and 147 (Table 8). The fragment ion at *m/z* 374 (loss of 176) suggested that M2 was a glucuronide conjugate. The ions at *m/z* 532 and 514, loss of one and two molecules of water, respectively, from the precursor ion suggested that the alcoholic hydroxyl groups were unsubstituted. The fragment ion at *m/z* 374, 46 Da (30+16) higher than the parent drug, further suggested the addition of a methoxy group and an oxygen atom to the molecule. The ions at *m/z* 176 and 147 indicated that

the oxidation had not occurred on the phenyl piperidine portion of the molecule and the fragment ions at *m/z* 181 and 163 suggested the presence of a methoxy group on phenylethyl portion of the molecule. Based on these data, M2 was tentatively assigned as the glucuronide conjugate of methoxy-hydroxy-TRX.

Metabolite M4. M4 had a retention time of 18.0-19.0 min on HPLC and was present in rat urine, bile and plasma. M4 showed a protonated molecular ion at *m/z* 550, 222 mass units higher than the parent molecule suggesting that it was a conjugate. The CID product ion spectrum of *m/z* 550 gave fragment ions at *m/z* 532, 374, 356, 206, 177, 162 and 151 (Table 8). The fragment ion at m/z 374, loss of 176 Da from the precursor ion indicated that it was a glucuronide conjugate. Further, the fragment ion at m/z 374 was appeared 46 Da higher than the parent ion suggesting the addition of a methoxy group and an oxygen atom to the molecule. The other prominent fragment ions at *m/z* 206, 177 and 162 suggested that the addition of 46 Da (OMe+OH-2H) had occurred on the phenyl piperidine portion of the molecule. The ion at *m/z* 151 suggested that the hydroxy-phenyl ring was unchanged. Based on these data, M4 was tentatively identified as glucuronide conjugate of methoxy-hydroxy-TRX**.**

Metabolite M5. M5 was present in both urine and feces of rats and showed a protonated molecular ion at *m/z* 360. The molecular ion at *m/z* 360, 32 Da higher than the parent drug was indicative of the addition of two oxygen atoms to the molecule. The CID product ion spectrum of *m/z* 360 gave fragment ions at *m/z* 342 $(MH\text{-}H_2O)^+$, 324 $(MH\text{-}H_2O\text{-}H_2O)^+$, 192, 163, 151 and 133 (Table 8). The characteristic ions at *m/z* 151 and 133 indicated that the hydroxy phenyl moiety was unchanged. The fragment ions at *m/z* 192 and 163 suggested that both the oxygen atoms had been added to the phenyl piperidine moiety. Based on these data, M5 was tentatively identified as dihydroxy-TRX.

Metabolite M6. Full scan MS of M6 displayed a protonated molecular ion at *m/z* 504, 176 Da higher than TRX suggesting that it was a glucuronide conjugate of the parent drug. The CID product ion spectrum of m/z 504 gave the fragment ions at m/z 486 $(MH\text{-}H_2O)^+$, 328 (MH-glucuronide)$^+$, 310 (MH-glucuronide-H_2O)$^+$, 292 (MH-glucuronide-H_2O-H_2O)$^+$, 160, 151 and 131 (Table 8). Based on these data, M6 was identified as the phenolic glucuronide of TRX (Johnson et al., 2003).

Metabolite M7. Full scan of M7 displayed a protonated molecular ion at *m/z* 534. The CID product ion spectrum of *m/z* 534 gave the intense ions at *m/z* 516 $(MH\text{-}H_2O)^+$, 358, 340, 181, 160 and 131 (Table 8). The fragment ion at *m/z* 358, loss of 176 Da from the precursor ion suggested that it was a glucuronide conjugate. The fragment ion at *m/z* 181 suggested the addition of a methoxy group on the hydroxy phenyl ring. The other prominent ion at *m/z* 160 suggested that the phenyl piperidine portion of the molecule was unsubstituted. Based on these data, M7 was tentatively identified as the glucuronide conjugates of methoxy-TRX.

Metabolite M8. M8 showed a protonated molecular ion at *m/z* 344, 16 Da higher than TRX, indicating the addition of an oxygen atom to the molecule. CID product ion spectrum of *m/z* 344 showed the fragment ions at 326 $(MH\text{-}H_2O)^+$, 308 $(MH\text{-}H_2O\text{-}H_2O)^+$, 176, 151, 147 and 133 (Table 8). The fragment ions at *m/z* 176 and 147 suggested the addition of an oxygen atom on the phenyl piperidine portion of the molecule. The prominent fragment ions at *m/z* 151 and 133 indicated that the hydroxy phenyl ring was unsubstituted. M8 had the same retention time and identical CID daughter spectrum as the synthetic standard (4'-hydroxy-TRX). Based on these data, M8 was identified as 4'-hydroxy-TRX.

Metabolite M9. Full scan MS of M9 displayed a protonated molecular ion at *m/z* 374, 46 Da higher than TRX, which was indicative of the addition of a methoxy group and an oxygen atom to the molecule. CID product ion spectrum of *m/z* 374 showed the fragment ions at *m/z* 356 $(MH\text{-}H_2O)^+$, 338 $(MH\text{-}H_2O\text{-}H_2O)^+$, 181, 176, 163 and 147 (Table 8). The fragment ion at *m/z* 176 and 147 suggested that the oxidation had occurred at the phenyl-piperidine part of the molecule. The other prominent fragment ions at *m/z* 181 and 163 suggested the presence of a methoxy group on the hydroxy phenyl ring. Based on these data, M9 was tentatively identified as the 3-methoxy hydroxy-TRX.

Metabolite M10. The protonated molecular ion at *m/z* 374, 46 Da higher than TRX, was indicative of the addition of a methoxy group and an oxygen atom to the molecule. CID product ion spectrum of *m/z* 374 showed fragment ions at *m/z* 356 $(MH\text{-}H_2O)^+$, 338 $(MH\text{-}H_2O\text{-}H_2O)^+$, 206, 177, 151, 145 and 133 (Table 8). The diagnostic fragment ions at *m/z* 151 and 133 suggested that the hydroxy phenyl ring was unsubstituted. The presence of fragment ions at *m/z* 206 and 177 indicated that the addition of methoxy group and an oxygen atom had occurred at the phenyl piperidine moiety. Based on these data, M10 was tentatively identified as the methoxy-hydroxy-TRX.

Metabolite M11. M11 had a retention time of 26.3 min on the HPLC and it was present in urine and bile of both male and female rats. M11 showed a protonated molecular ion at *m/z* 344, 16 Da higher than the drug, suggesting the addition of an oxygen atom to the molecule. The CID product ion spectrum of *m/z* 344 showed fragment ions at m/z 326 $(MH\text{-}H_2O)^+$, 308 $(MH\text{-}H_2O\text{-}H_2O)^+$, 176, 151 and 147 (Table 8). The significant and distinct fragment ions at *m/z* 176

and 147 suggested that the hydroxylation had occurred on the phenyl ring attached to the piperidine ring. The fragment ions at *m/z* 151 and 133 indicated that the hydroxy phenyl ring was unsubstituted. Based on these data, M11 was tentatively identified as the hydroxy-TRX.

Metabolite M12. M12 showed a protonated molecular ion at *m/z* 344, 16 Da higher than the parent drug, indicating the addition of an oxygen atom to the molecule. The CID product ion spectrum of *m/z* 344 showed the fragment ions at *m/z* 326 $(MH\text{-}H_2O)^+$, 308, 178, 167, 160, 149 and 131 (Table 8). The fragment ions at m/z 178 and 160 suggested that the phenyl-piperidine moiety was unchanged. The fragment ion at *m/z* 167 and 149 indicated that the oxidation had occurred on the hydroxy-phenyl ring. M12 showed similar HPLC retention time and identical CID daughter spectrum as the synthetic 3-hydroxy-TRX. Based on these data, M12 was identified as 3-hydroxy-TRX.

Metabolite M13. M13 was present only in urine and plasma of both rats and dogs. M13 showed a protonated molecular ion at *m/z* 358, 30 Da higher than the parent TRX, indicating that a methoxy group had been added to the molecule. The CID product ion spectrum of *m/z* 358 gave intense ions at *m/z* 340 $(MH\text{-}H_2O)^+$, 322 $(MH\text{-}H_2O\text{-}H_2O)^+$, 181, 160, 151 and 131 (Table 8). The fragment ions at *m/z* 160 and 131 suggested the phenyl piperidine moiety was unchanged. The ions at *m/z* 181 and 151 indicated that the methoxy group had been added to the phenyl-ethyl portion of the molecule. M13 showed similar retention time and identical CID daughter spectrum as the synthetic standard 3-methoxy-TRX. Based on these data, M13 was identified as 3-methoxy-TRX (Johnson et al., 2003).

Metabolite M14. M14 had a retention time of ~26:40 min on the HPLC and was found only in urine and bile of dogs. It showed a protonated molecular ion at *m/z* 438, 110 Da higher than the parent molecule, suggesting that it was a conjugate. The CID product ion spectrum of *m/*z 438 gave intense fragment ions at *m/*z 358, 340, 181 and 160 (Table 8). The fragment ion at *m/z* 358, loss of 80, suggested that M14 was a sulfate conjugate. The fragment ions at *m/z* 181 and 151 indicated that a methoxy group had been added to the hydroxy phenyl ring of the molecule. The fragment ion at *m/z* 160 suggested that the phenyl piperidine moiety was unchanged. Based on these data, M14 was identified as the sulfate conjugate of 3-methoxy-TRX.

Discussion

We report the metabolic fate and disposition of [^{14}C]TRX after i.v. administration to rats and dogs, the animal species used for safety toxicology studies. The administered radioactive dose was quantitatively recovered from the urine and feces of both rats (92%) and dogs (88%) over a period of 120-168 h. Essentially the entire administered dose was recovered within 48 h in both species, suggesting rapid excretion of the TRX radioactivity. The urinary excretion of the radioactivity was somewhat higher in the females compared to males for both rats (41 and 21%) and dogs (48 and 30%). In contrast, the fecal recoveries in males (rats 71%; dogs 53%) were somewhat higher than in the females (rats 52%; dogs 46%). The gender-related differences in the elimination and pharmacokinetics of xenobiotics, especially for rats, have been well known and can be result of the differences in hormone levels, plasma protein binding, and/or rate and extent of metabolism (Tanaka et al., 1991a, 1991b; Prakash and Soliman, 1997). Because a substantial portion of the radioactivity was also recovered in the feces of rats (61%) and dogs (49%) following i.v. dose, suggesting that TRX is eliminated via both biliary and urinary routes in these animal species.

The distribution of [^{14}C]TRX radioactivity was short-lived in most tissues of LE rats. A rapid elimination of the parent drug and metabolites for the majority of tissues in the female and male rats was evident by the lack of drug radioactivity by 3 h following an i.v. dose. There were no apparent gender-related differences in the distribution of [^{14}C]TRX radioactivity in rats. Sufficient concentrations of TRX radioactivity were present for quantification mainly at earlier time points and in the uvea, liver, kidney, and GIT contents at later times. The uvea, kidney and liver were the only tissues with sustained concentrations of [^{14}C]TRX radioactivity after 8 h post dose. By 168 h only the uvea had measurable concentrations of drug radioactivity. Association of [^{14}C]TRX radioactivity with the uvea resulted from the affinity of melanin-rich tissues for organic amines and polycyclic aromatic hydrocarbons. The retention or accumulation of xenobiotics having cationic properties by ocular tissues impregnated with melanin appears to be common (Larsson and Tjalve, 1979). Mean plasma concentrations unchanged TRX at the first time point were slightly higher in females than in males for both rats and dogs. Similarly, AUC values of unchanged TRX and total radioactivity in both rats and dog were also slightly higher for females than males, suggesting that females have higher exposure of TRX and metabolites compared to males. The terminal phase $T_{1/2}$ for total radioactivity was longer than for TRX itself in both rat and dogs. It could be either a long lived metabolite or covalent binding of radioactivity. We had the similar findings in humans where the half life of total radioactivity was several fold higher than parent compound (Johnson et al., 2003).

The urine and bile radiochromatograms from rats and dogs indicate that TRX is readily metabolized before excretion. The major portion of administered radioactivity was excreted in urine and bile as conjugates of parent drug and its hydroxylated metabolites. There were no sex

related qualitative differences in the profile of metabolites. However, there were notable species related qualitative and quantitative differences in the metabolic profiles. A total of 13 metabolites in rats and 7 metabolites in dogs were identified by ion spray LC/MS/MS, a very soft ionization technique that has allowed the identification of polar phase II metabolites (Kamel and Prakash, 2006; Prakash et al., 2007). The structures of several metabolites were confirmed unambiguously by comparison of their chromatographic and mass spectral fragmentation properties with those of the synthetic standards. Other metabolites were tentatively identified based on their fragmentation patterns. A proposed scheme for the biotransformation pathways of TRX in rats and dogs is shown in Fig 1. Based on the structures of the metabolites, three primary metabolic pathways of TRX were identified: hydroxylation at the phenol ring, hydroxylation at the aromatic ring attached to piperidine and conjugation with glucuronic acid. Metabolites presumably derived from these routes were found to be capable of undergoing further metabolism by various combinations of the primary routes and methylation of the catechol intermediate by catechol-O-methyl transferase and subsequent phase II conjugation. The metabolic pathways of TRX in dogs were similar to those observed in humnas (Johnson et al., 2003). With respect to hydroxylating capacity the rat has a broader spectrum of metabolites as this species is capable of hydroxylating both the aromatic rings, whereas, in dogs hydroxylation is favored at the phenol. This pathway was also found to be the major pathway for the structurally similar drug, ifenprodil (Durand et al., 1981). However, for TRX, oxidation at the phenyl ring attached to piperidinol was observed as the major metabolic pathway in rats.

The major components of drug related material in rat excreta were identified as 4'-hydroxy-TRX (M8), 3-hydroxy-TRX (M12), 3-methoxy-4'-hydroxy-TRX (M9) and their glucuronide conjugates (M1, M2 and M3) and TRX glucuronide (M6). Unchanged drug (36%) and its

glucuronide conjugate (M6, 35%) were identified as major circulating metabolites in both male and female rats. The full scan LC-MS of metabolites, M8, M11 and M12 displayed protonated molecular ions at *m/z* 344, suggesting that these metabolites were monooxygenated and regioisomers. The fragment ions in the CID product ion spectra of M8 and M12 were able to define the site of hydroxylation at the phenyl-piperidinol and phenol moieties, respectively. However the MS-MS spectra did not provide the exact position of the hydroxy group. Therefore, these two regioisomers were synthesized (Fig. 2). The structures of M8 and M12 were characterized unambiguously by comparison of their chromatographic properties and CID spectra with those of synthetic standards. Similarly, the full scan MS of metabolites M1 and M3 displayed protonated molecular ions at *m/z* 520, suggesting that both these metabolites were glucuronide conjugates of hydroxy metabolites and were positional isomers. Further MS/MS spectra of M1 and M3 suggested that these were glucuronide conjugates of 4'-hydroxy-TRX. The site of conjugation was established by comparison of retention time and CID mass spectra of metabolites with synthetic glucuronide conjugates, obtained by *in vitro* incubation 4'-hydroxy-TRX with PB induced rat liver microsomes in the presence of UDPGA. Two glucuronide conjugates were obtained from the *in vitro* incubation of 4'-hydroxy-TRX. The position of glucuronide was established at the phenolic hydroxyl group from the differences in the CID product ion spectra of methylated products of 4'-hydroxy-TRX, and its glucuronide conjugate. No alcoholic glucuronide was detected in urine, bile or *in vitro* incubations.

Unlike rats, the major components of drug related material in the dog bile were identified as 3-methoxy-TRX (M9) and its glucuronide (M7) and sulfate conjugate (M14). 3-Methoxy-TRX (M9) and its glucuronide (M7) were also identified as the major metabolites in humans (Johnson et al., 2003). Sulfate conjugate M14, however, was not detected in rats. There are a number of

compounds that demonstrate similar species specificity for the formation of O-sulfate conjugate in dogs compared with rodents. For example, denopamine (Furuuchi et al 1985) and 4-hydroyatomoxetine (Mattiuz et al., 2003) undergo either O-sulfation (dog only) or O-glucuronidation (dog and rodent). Morgan et al. (1969) reported that isoproterenol, structurally similar to 3-hydroxy-TRX, metabolized to 3-O-methylisoproterenol and its sulfate conjugate in humans. Unchanged drug and metabolite M13 (76%) were identified as the major circulating drug related material in both male and female dogs.

In summary, the results of this study provide the first analysis of formation and excretion of metabolites of TRX in rats and dogs, two species used in toxicology studies. TRX is extensively metabolized in both rats and dogs after i.v. administration and the radioactive dose is excreted mainly in urine and feces via bile. TRX is eliminated by both Phase I and Phase II metabolism. There were notable species-related qualitative and quantitative differences in the metabolism of TRX in rats and dogs. Similar to humans, the hydroxylation at the 3-position of the phenol ring followed by methylation of the resulting catechol intermediate and subsequent conjugation were identified as the main metabolic pathways of TRX in dogs. In contrast, the major metabolites in rats were due to oxidation at the phenylpiperidinol moiety followed by glucuronide conjugation.

Acknowledgments. We would like to thank Dr. Kathleen Zandi and Ms. Sandra Miller for providing radiolabelled TRX, Mr. Clinton M. Schroeder for the acquisition of cryosections and electronic images and Ms. Kim Johnson and Ms. Beth Obach for technical assistance.

References

Albin RL, Greenamyre JT (1992) Alternative excitotoxic hypothesis Neurol **42**:733-737.

Baillie TA, Cayen MN, Fouda H, Gerson RJ, Green JD, Grossman SJ, Klunk LJ, LeBlanc B, Perkins DG, Shipley LA (2002) Drug Metabolites in Safety Testing. *Toxicol Appl Pharmacol* **182:**188-196.

Bullock R, Kuroda Y, Teasdale GM, NcCulloch J (1992) Prevention of post-traumatic excitotoxic brain damage with NMDA antagonist drug: a new strategy for the nineties. *Acta Neurochir* **55**:49-55.

Bullock MR, Merchant RE, Carmack CA, Doppenberg E, Shah AK, Wilner KD, Ko G, Williams SA (1999) An open-label study of CP-101,606 in subjects with a severe traumatic head injury or spontaneous intracerebral hemorrhage. *Ann New York Acad Sci* **890**:51-58.

Chazot L (2000) CP-101606 (Pfizer Inc). *Curr Opin Invest Drugs* **1(3)**:370-374.

Chazot PL (2004) The NMDA receptor NR2B subunit: A valid therapeutic target for multiple CNS pathologies. *Curr Med Chem* **11(3):**389-396.

Chenard BL, Shalaby IA, Koe BK, Ronau RT, Butler TW, Prochniak MA, Schmidt AW, Fox CB (1991) Separation of α1-adrenergic and N-methyl-D-aspartate antagonist activity in a series of ifenprodil compounds. *J Med Chem* **34**:3085-3090.

Chenard BL, Bordner J, Butler TW, Chambers LK, Collins MA, De Costa DL, Ducat MF, Dumont ML, Fox CB, Mena EE, Menniti FS, Nielsen J, Pagnozzi MJ, Richter KEG, Ronau RT, Shalaby IA, Stemple JZ, White WF (1995) (1S, 2S)-1-(4-hydroxy-phenyl)-2-(4-hydroxy-4-phenyl-piperidino)-1-propanol: A potent new neuroprotectant which blocks of N-methyl-D-aspartate responses. *J Med Chem* **38**:3138-3145.

Di X, Bullock R, Watson J, Fatouros P, Chenard B, White W and Corwin F (1997) Effect of TRXL, a novel NR2B subunit antagonist of N-methyl-D-aspartate receptor, on the volume of ischemic brain damage and cytotoxic brain edema after cerebral artery occlusion in the feline brain. *Stroke* **28**:2241-2251.

Durand A, Ferrandes B, Morselli P, Synthelabo L (1981) Pharmacokinetics of ifenprodil and its major metabolites in the male and female rats. *Eur cong Biopharm Pharmacokinet* **1**:136-142.

Furuuchi S, Naito K, Otsuka M, Harigaya S (1985) Metabolism of denopamine, a new cardiotonic agent, in the rat and dog. *Drug Metab Dispos* **13**:620-626

Green JG, Greenamyre JT (1996) Bioenergetics and glutamate excitotoxicity. *Prog Neurobiol* **48**:613-634.

Guzikowski AP, Tamiz A P, Acosta-Burruel M, Hong-Bae S, Cai SX, Hawkinson JE, Keana JFW, Kesten SR, Shipp CT, Tran M, Whittemore ER, Woodward RM,Wright JL, Zhou ZL (2000) Synthesis of N-Substituted 4-(4-Hydroxyphenyl)piperidines, 4-(4-hydroxybenzyl)piperidines, and (±)-3-(4-Hydroxyphenyl)pyrrolidines: Selective Antagonists at the 1A/2B NMDA Receptor Subtype. *J Med Chem* **4**:984-994.

Johnson K, Shah A, Jaw J, Baxter J, Prakash C (2003) Metabolism, pharmacokinetics, and excretion of a highly selective NMDA receptor antagonist, traxoprodil, in human cytochrome P450 2D6 extensive and poor metabolizers. *Drug Metab Dispos* **31**:76-87.

Kamel A, Prakash C (2006) High performance liquid chromatography/atmospheric pressure ionization /tandem Mass spectrometry (HPLC/API/MS/MS) in drug metabolism and toxicology studies. *Curr Drug Metab* **7**:837-852.

Larsson B, Tjalve H (1979) Studies on the mechanism of drug-binding to melanin. *Biochem Pharmacol* **28**:1181-1187.

Maragos WF, Greenamyre JT, Penney, JB and Young AB (1987) Glutamate dysfunction in Alzheimer,s disease:an hypothesis. *Trends Neurosci* **10**:65-68.

Mattiuz EL, Ponsler GD, Barbuch RJ, Wood PG, Mullen JH, Shugert RL, Li Q, Wheeler WJ, Kuo F, Conrad PC, Sauer JM (2002) Disposition and metabolic fate of atomoxetine

hydrochloride: pharmacokinetics, metabolism, and excretion in the Fischer 344 rat and beagle dog. *Drug MetabDispos* **31(1):**88-97.

McCarthy KE, Miller SA, Chenard BL, Butler TW, Dumont ML, Stemple JZ (1997) Synthesis of high specific activity tritium and optically pure [^{14}C]CP-101,606. Enantioselective crystalization of a radiochemically racemic mixture. *J labelled Comp Radiopharm* **39**:973-985.

Menniti FS, Chenard BL, Collins MA, Ducat MF, Shalaby IA and White WF (1997) CP-101,606: A potent neuroprotectant selective for forebrain neurons. *Eur J Pharmacol* **331**:117-126

Menniti FS, Shah AK, William SA, Wilner KD, White WF, Chenard BL (1998) CP-101,606: An NR2B-selective NMDA receptor antagonist. *CNS Drug Rev* **4**:307-322.

Menniti FS, Pagnozzi MJ, Butler P, Chenard BL, Jaw-Tsai S, White WF (2000) CP-101,606, an NR2B subunit selective NMDA receptor antagonist inhibits NMDA and injury induced c-fos expression and cortical spreading depression in rodents. *Neuropharmacol* **39**:1147-1155.

Merchant RE, Bullock R, Carmack CA, Shah A, Wilner K, Ko G, Williams S A (1999). A double-blind placebo-controlled trial of TRX in patients with mild or moderate traumatic brain injury. *Ann NY Acad Sci* **890**:42-50.

Morgan D, Sandler M, Davies S, Conolly M, Paterson J, Dolley CT (1969) Metabolic fate of DL-isoprenaline 7-^{3}H in man and dog. *Biochem J* **114**:8P

Palmer GC (2001) Neuroprotection by NMDA receptor antagonists in a variety of neuropathologies. *Curr Drug Targets* **2(3):**241-271.

Potchoiba MJ, Tensfeldt TG, Nocerini MR, Silber BM (1995) A novel quantitative method for determining the biodistribution of radiolabeled xenobiotics using whole-body cryosectioning and autoradioluminography. *J Pharmacol and Exp Ther* **272(2):** 953-962

Potchoiba MJ, West M, Nocerini MR (1998) Quantitative comparison of autoradioluminographic and radiometric tissue distribution studies using carbon-14 labeled xenobiotics. *Drug Metab and Dispos* **26**:272-277.

Prakash C , Soliman V (1997) Metabolism and excretion of a new anxiolytic drug candidate, CP-93,393, in Long-Evans rats. *Drug Metab Dispos* **25**:1288-1297.

Prakash C, Shaffer C, Nedderman A (2007) Analytical strategies for identifying drug metabolites. Mass Spectrom Rev **26**:340-369.

Tanaka Y, Deguchi Y, Ishi I, Terai T (1991a) Sex diffrences in excretion of zenarestat in rat. Xenobiotica **21**:1119-1125.

Tanaka Y, Kadoh Y, Mukumoto S, Ishikawa H (1991b) The role of age and sex hormones on the urinary excretion of zenarestat in rats. Xenobiotica **21**:1273-1279.

Tsuchida E, Rice M, Bullock R (1997) The neuroprotective effect of the forebrain-selective NMDA antagonist TRX upon focal ischemic brain damage caused by acute subdural hematoma in the rat. *J Neurotrauma* **14**:409-417

Ullberg S (1977) The technique of whole-body autoradiography cryosectioning of large specimens. *Science Tools The LKB Journal* 1-29,

Wood PL, Hawkinson JE (1997) N-methyl-D-aspartate antagonists for stroke and head trauma. *Expert Opin Invest Drugs* **6(4):**389-397.

DMD Fast Forward. Published on May 11, 2007 as DOI: 10.1124/dmd.107.016105
This article has not been copyedited and formatted. The final version may differ from this version.

Footnotes:

Send reprints requests to: Chandra Prakash, Ph. D., Department of Pharmacokinetics, Dynamics and Metabolism, Pfizer Global Research and Development, Groton, CT 06340. Email:Chandra.prakash@pfizer.com

Figure Legends:

Fig. 1. Proposed biotransformation pathways of [^{14}C]TRX in rats and dogs

Fig. 2 Synthetic steps for the synthesis of metabolites.

Fig.. 3. Mean plasma concentration-time curves of TRX and total radioactivity in Sprague-Dawley rats after a single 15 mg/kg i.v. dose of [^{14}C]TRX.

Fig..4. Mean plasma concentration-time curves of TRX and total radioactivity in dogs after a single 5 m/kg i.v. dose of [^{14}C]TRX.

Fig.. 5. HPLC-radiochromatograms of TRX metabolites in urine (0-48 h) and feces (0-48 h) of rats after a single i.v. dose of [^{14}C]TRX.

Fig. 6. HPLC-radiochromatograms of TRX metabolites in bile (0-8 h) and plasma (1 and 4 h) of rats after a single i.v. dose of [^{14}C]TRX.

Fig. 7. HPLC-radiochromatograms of TRX metabolites in urine (0-48 h) and feces (0-48 h) of dogs after a single i.v. dose of [^{14}C]TRX.

Fig. 8. HPLC-radiochromatograms of TRX metabolites in bile (0-8 h) and plasma (0-24 h) of dogs after a single i.v. dose of [^{14}C]TRX.

Fig. 9. CID product ion mass spectra of metabolite M1 (a) before (*m/z* 520) and (b) after treatment with diazomethane (*m/z* 548).

Fig. 10. CID product ion mass spectra of metabolite M3 (a) before (*m/z* 520) and (b) after treatment with diazomethane (*m/z* 548).

TABLE 1A

Mean percentage dose excreted in urine and feces from rats following i.v. administration of [^{14}C]TRX

Hours Post Dose	Male Rats (n=4)			Female Rats (n=4)			Mean		
(h)	Urine	Feces	Total	Urine	Feces	Total	Urine	Feces	Total
0-24	19.5	50.1	69.6	31.5	25.3	56.8	25.5	37.7	63.2
24-48	1.23	16.7	17.9	5.02	6.37	11.4	3.13	11.5	14.7
48-72	0.33	2.03	2.36	1.95	3.77	5.72	1.14	2.90	4.04
72-96	0.25	0.6	0.85	1.22	8.29	9.51	0.74	4.45	5.18
96-168	0.19	1.12	1.31	1.33	8.03	9.36	0.76	4.58	5.34
0-168	21.6	70.5	92.1	41.0	51.7	92.7	31.3	61.1	92.4

TABLE 1B

Mean percentage dose excreted in urine and feces from dogs following i.v. administration of [^{14}C]TRX

Hours Post Dose	Male Dogs (n=2)			Female Dogs (n=2)			Mean		
(h)	Urine	Feces	Total	Urine	Feces	Total	Urine	Feces	Total
0-24	24.7	38.9	63.6	43.5	37.7	81.2	34.1	38.3	72.4
24-48	3.86	12.0	15.86	3.4	6.69	10.1	3.64	9.35	13.0
48-72	0.59	1.13	1.72	0.73	1.23	1.96	0.66	1.18	1.84
72-96	0.29	0.62	0.91	0.37	0.26	0.63	0.33	0.44	0.77
96-120	0.21	ND	0.21	0.18	ND	0.18	0.20	ND	0.20
0-120	29.7	52.7	82.4	48.2	45.9	94.1	38.9	49.3	88.2

DMD Fast Forward. Published on May 11, 2007 as DOI: 10.1124/dmd.107.016105
This article has not been copyedited and formatted. The final version may differ from this version.

TABLE 2

Mean pharmacokinetic parameters for TRX and total radioactivity in rats and dogs following i.v. administration of [^{14}C]TRX

Analyte	Species	$T_{1/2}$ (h)	C_{max} (ng/ml)	$AUC_{(0-t)}$ (ng.h/ml)	$AUC_{(0-\infty)}$ (ng.h/ml)
Parent	Male rat	1.36	416	386	388
	Female rat	1.70	683	624	626
	Mean	1.53	550	505	507
	Male dog	5.61	418	1570	1620
	Female dog	4.48	585	2500	2550
	Mean	5.0	502	2040	2090
Radioactivity *	Male rat	8.08	1470	3440	-
	Female rat	9.07	1750	3730	-
	Mean	8.6	1610	3590	
	Male dog	43.1	1570	26000	-
	Female dog	38.2	1750	32200	-
	Mean	40.7	1660	29100	

*C_{max} and AUC values for total radioactivity are expressed as ng-eq/ml and ng-eq.h/ml, respectively.

TABLE 3

Tissues concentration of [^{14}C]TRX radioequivalents (mean ±S.D., nCi/g) for male rats following i.v. administration of [^{14}C]TRX[a].

	Male Long-Evans Rats					Female Long-Evans Rats				
Tissue	0.33 h	3 h	8 h	24 h	168 h	0.33 h	3 h	8 h	24 h	168 h
Adipose: Brown	41	nd	nd	nd	nd	49	nd	nd	nd	nd
Adipose: White	<lloq[c]	<lloq	<lloq	<lloq	<lloq	<lloq	<lloq	<lloq	<lloq	<lloq
Bone Marrow: Femur	93	nd	nd	nd	nd	109	nd	nd	nd	nd
Bone Marrow: Vertebrae	74	nd	nd	nd	nd	83	nd	nd	nd	nd
Brain	22	nd[b]	nd	nd	nd	28	nd	nd	nd	nd
Choroid	nd	nd	249	152	54	297	250	235	216	80
Ciliary Body	nd	nd	383	202	105	450	369	271	352	137
Colon Contents	nd	31	614	280	nd	nd	nd	nd	52	nd
Gastric Contents	385	26	nd	6	nd	219	nd	nd	nd	nd
Harderian Gland	128	nd	nd	nd	nd	nd	nd	nd	nd	nd
Intestinal Contents	2170	711	161	71	nd	360	947	405	24	10
Iris	nd	nd	144	157	46	83	121	159	258	79
Kidney	122	19	13	9	nd	111	22	13	9	lloq
Lacrimal Gland	133	16	8	nd	nd	153	12	8	nd	nd
Liver	205	49	12	9	nd	161	43	17	9	nd
Lung	56	nd	nd	nd	nd	72	nd	nd	nd	nd
Myocardial Blood	14	nd	nd	nd	nd	17	nd	nd	nd	nd
Myocardium	33	nd	nd	nd	nd	42	nd	nd	nd	nd
Pancreas	nd	42	nd	nd	nd	nd	47	nd	nd	nd
Salivary Gland	106	10	<lloq	<lloq	<lloq	181	12	11	nd	nd
Skeletal Muscle	44	nd	nd	nd	nd	58	lloq	nd	nd	nd
Spleen	91	<lloq	nd	nd	nd	93	21	lloq	nd	nd
Testes	16	16	8	<lloq	nd	-----	-----	-----	-----	-----
Thymus	56	nd	nd	nd	nd	75	nd	nd	nd	nd
Uvea	339	219	219	154	53	290	233	248	220	65

[a]Mean tissue radioactivity concentrations (nCi/g) were calculated by averaging tissue concentrations measured at different sectioning levels and/or from replicate cryosections obtained from the same sectioning level.
[b]Concentration not determined due to tissue identification not distinguishable from background.
[c]Concentration was below the lower limit of quantitation (lloq) of 5.9 nCi/g.

.

TABLE 4

Mean percentage of the dose of urinary and fecal metabolites of TRX in male and female rats following i.v. administration of [^{14}C]TRX*

Metabolite (#)	Retention Time (min)	% of Dose								
		Male Rats			Female Rats			Mean		
		Urine	Feces	Total	Urine	Feces	Total	Urine	Feces	Total
M1	13.07	0.46	nd	0.46	0.88	0.00	0.88	0.67	nd	0.67
M2	14.97	0.30	nd	0.30	0.56	0.00	0.56	0.43	nd	0.43
M3	15.88	1.14	nd	1.14	2.18	0.00	2.18	1.66	nd	1.66
M4	19.02	0.29	nd	0.29	0.55	0.00	0.55	0.42	nd	0.42
M5	20.42	0.19	29.8	30.0	0.37	23.2	23.57	0.28	26.5	26.8
M6	21.25	5.15	nd	5.15	9.80	nd	9.80	7.48	0.00	7.48
M7	22.83	0.50	nd	0.50	0.95	nd	0.95	0.72	0.00	0.72
M8	23.93	4.28	20.2	24.5	8.13	12.3	20.4	6.20	16.2	22.4
M9	24.83	0.27	1.08	1.35	0.52	1.71	2.22	0.39	1.39	1.79
M10	25.77	0.66	3.54	4.20	1.26	4.48	5.74	0.96	4.01	4.97
M11	26.35	0.17	nd	0.17	0.32	nd	0.32	0.24	0.00	0.24
M12	28.27	0.17	2.71	2.88	0.33	nd	0.33	0.25	1.35	1.60
TRX	30.72	5.65	1.83	7.48	10.74	1.57	12.32	8.20	1.70	9.90
M13	31.57	0.16	nd	0.16	0.30	3.13	3.43	0.23	1.57	1.79

*The relative abundance of metabolites is based on the amount of radioactivity excreted in urine and feces
nd= not detected

TABLE 5

Mean percentage of biliary metabolites of TRX in rats and dogs following i.v. administration of [^{14}C]TRX*

Metabolite	Retention Time	Percent of Total Bile Radioactivity					
		Rats			Dogs		
(#)	(min)	Male	Female	Mean	Male	Femal e	Mean
M1	13.07	5.44	5.00	5.22	nd	nd	na
M2	14.97	10.4	7.43	8.90	nd	nd	na
M3	15.88	13.9	8.21	11.0	nd	nd	na
M4	19.02	7.35	0.24	3.80	nd	nd	na
M5	20.42	4.17	nd	2.09	nd	nd	na
M6	21.25	12.9	23.3	18.1	6.42	4.34	5.38
M7	22.83	nd	17.9	8.96	46.8	27.6	37.2
M8	23.93	18.9	11.3	15.1	2.9	2.28	2.59
M9	24.83	3.40	1.58	2.49	nd	nd	na
M10	25.77	8.09	2.84	5.47	nd	nd	na
M11	26.35	1.16	2.30	1.73	2.69	2.11	2.4
M12	28.27	2.69	0.28	1.49	nd	nd	na
TRX	30.72	0.35	1.91	1.13	20.9**	17.3**	19.1**
M13	31.57	nd	nd	nd	-	-	-
M14	26.67	nd	nd	nd	8.47	35.5	22.0

DMD Fast Forward. Published on May 11, 2007 as DOI: 10.1124/dmd.107.016105
This article has not been copyedited and formatted. The final version may differ from this version.

*The relative abundance of metabolites is based on the amount of radioactivity excreted in bile
nd=not detected; na=not applicable

**A mixture of TRX and M13

DMD Fast Forward. Published on May 11, 2007 as DOI: 10.1124/dmd.107.016105
This article has not been copyedited and formatted. The final version may differ from this version.

TABLE 6

Mean percentage of circulating metabolites of TRX in rats and dogs following i.v. administration of [^{14}C]TRX*

Metabolite (#)	Retention Time (min)	Rats			Dog		
		Male	Female	Mean	Male	Female	Mean
M3	16.68	2.54	5.81	4.18	nd	nd	na
M4	18.05	5.62	2.44	4.03	nd	nd	na
M6	20.54	31.9	39.1	35.5	0.36	0.38	0.37
M7	20.75	3.30	3.71	3.51	3.54	2.93	3.24
M8	22.40	2.93	2.17	2.55	nd	nd	na
M10	24.47	0.67	1.22	0.95	nd	nd	na
TRX	29.28	36.5	33.7	35.1	72.8**	77.5**	75.2**
M13	29.28	0.72	1.37	1.05	-	-	-
M14	25.52	nd	nd	na	3.18	3.13	3.16

*The relative abundance of metabolites is based on the amount of radioactivity present in plasma
nd=not detected; na=not applicable

** Mixture of TRX+M13

TABLE 7

Mean percentage of the dose of urinary and fecal metabolites of TRX in male and female dogs following i.v. administration of [^{14}C]TRX*

Metabolite (#)	% of Dose								
	Male Dogs			Female Dogs			Mean		
	Urine	Feces	Total	Urine	Feces	Total	Urine	Feces	Total
M6	0.5	nd	0.5	0.8	nd	0.8	0.65	nd	0.65
M7	1.6	nd	1.6	2.0	nd	2	1.8	nd	1.8
M8	0.4	nd	0.4	0.4	nd	0.4	0.4	nd	0.4
M11	0.2	2.4	2.6	0.1	1.6	1.7	0.15	2.0	2.15
M12	nd	10.3	10.3	nd	5.6	5.6	nd	7.95	7.95
TRX	12.0**	9.0	21.0	18.6**	16.9	35.5	15.3**	13.0	28.3
M13	-	22.6	22.6	-	23	23	-	22.8	22.8
M14	8.7	nd	8.7	19.1	nd	19.1	13.9	0	13.9

*The relative abundance of metabolites is based on the amount of radioactivity excreted in urine and feces

nd=not detected; * *Mixture of TRX+ M13

TABLE 8
Major CID product ions of proposed metabolites of TRX

Metabolite	Structure	MH^+	Fragment ions
TRX	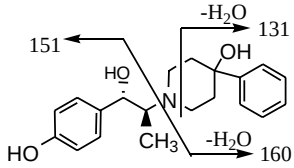	328	310, 174, 160,151,133 and 131
M1	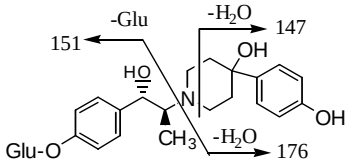	520	502, 326 ,176,151 and 147
M2	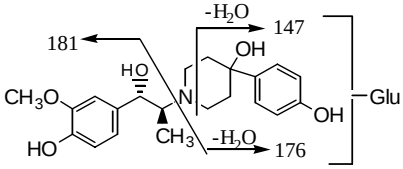	550	532, 514, 374, 356, 181, 176, 163 and 147
M3	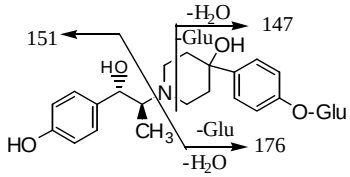	520	502, 484, 344, 326 ,176,151 and 147
M4	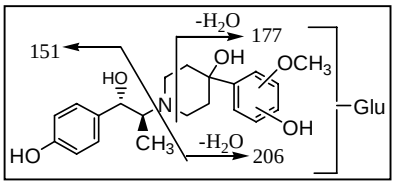	550	532, 374, 356, 206, 177, 162 and 151
M5	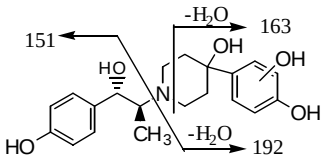	360	342, 324, 192, 163,151 and 133
M6	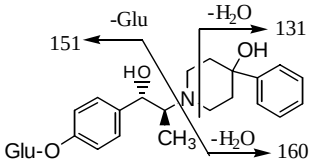	504	486, 328, 310, 292, 160, 151 and 131

DMD Fast Forward. Published on May 11, 2007 as DOI: 10.1124/dmd.107.016105
This article has not been copyedited and formatted. The final version may differ from this version.

M7	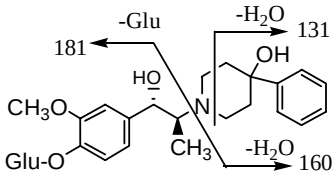	534	516, 358, 340, 181, 160 and 131
M8	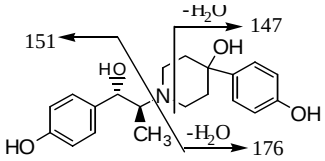	344	326, 308, 176, 151, 147 and 133
M9	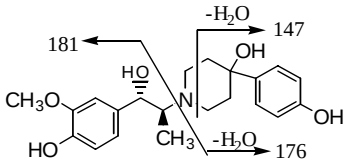	374	356, 338, 181, 176, 163 and 147
M10	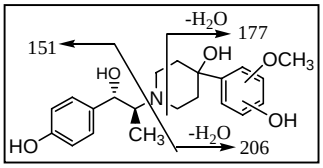	374	356, 338, 206, 177, 151, 145 and 133
M11	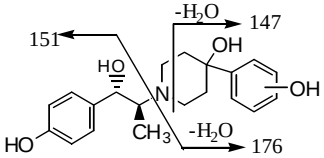	344	326, 308, 176, 151, 147 and 133
M12	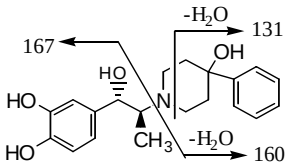	344	326, 308,178, 167, 160, 149 and 131
M13	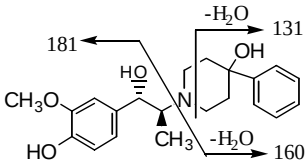	358	340, 322, 181, 160, 151 and 131
M14	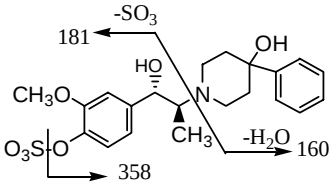	438	358, 340, 181 and 160

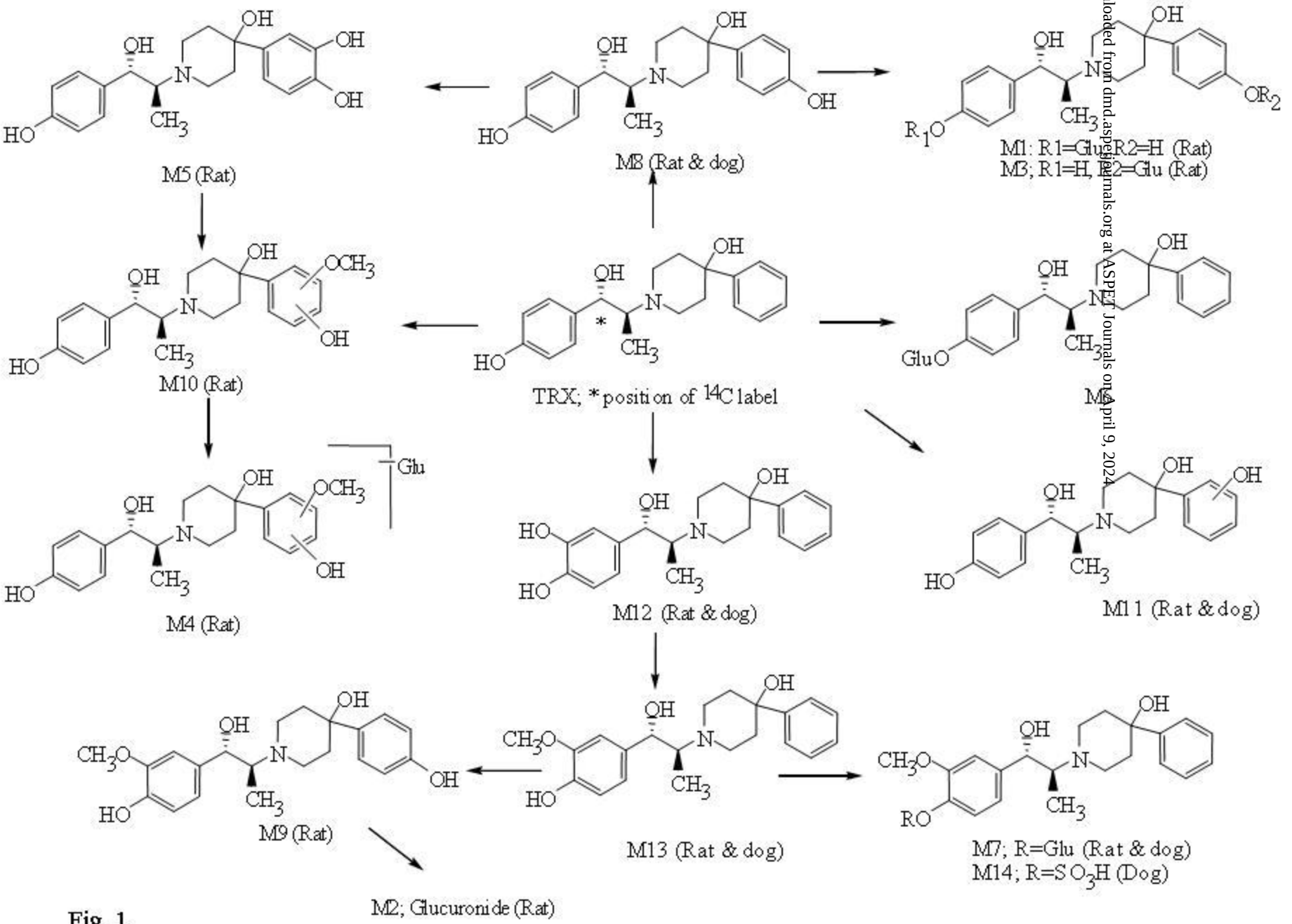

Fig. 1

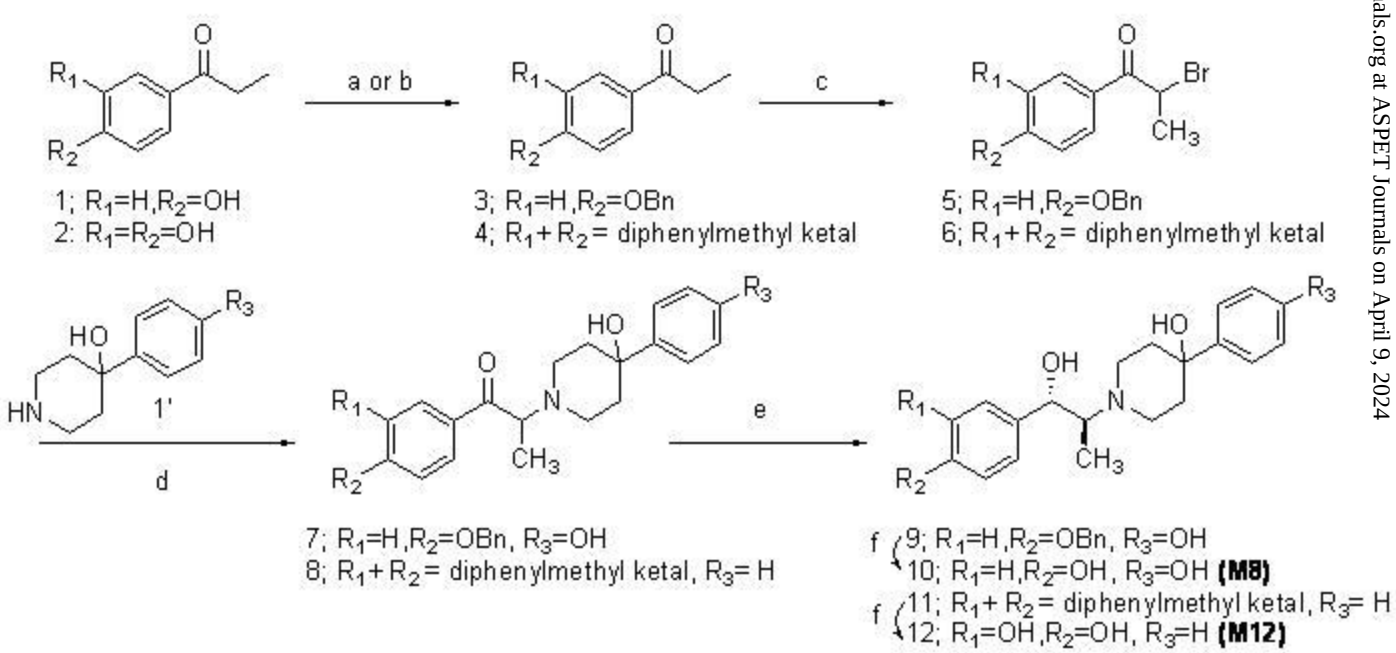

Reagents: (a) Bn (benzyl)Br, K_2CO_3, acetone; (b) dichlorodiphenylmethane, 170C; (c) Br_2, CCl_4; (d) Et_3N, EtOH; (e) $NaBH_4$, EtOH; (f)H_2, 10% Pd/C, MeOH, HOAc

Fig. 2

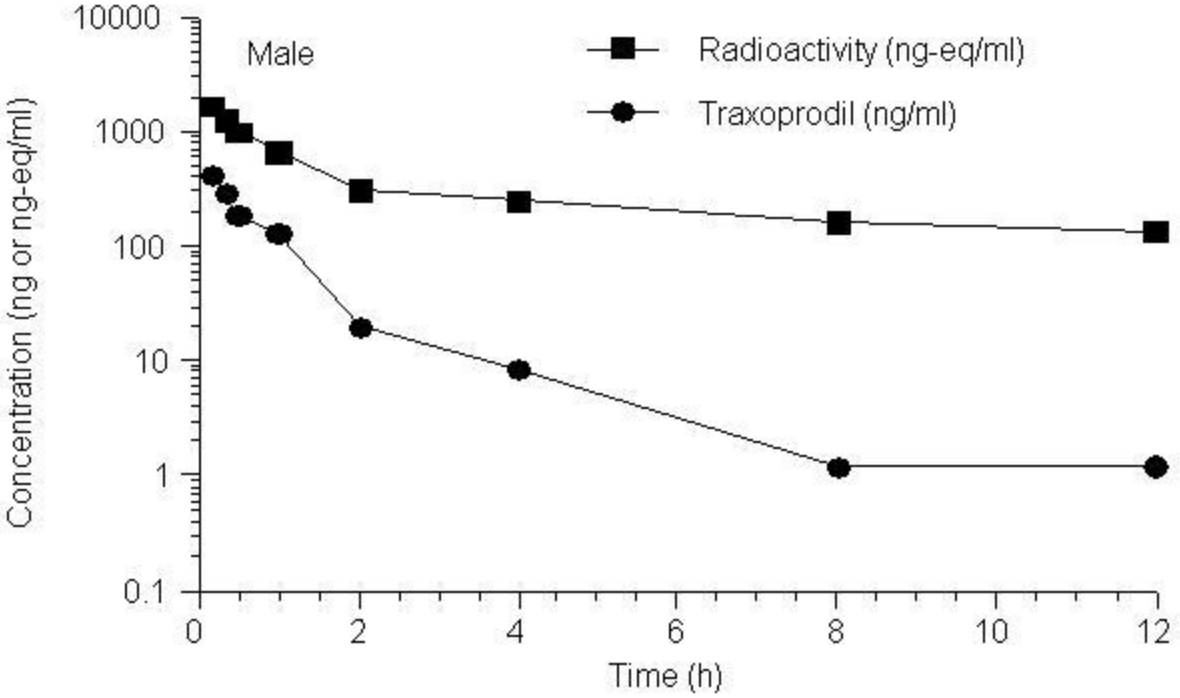
Male
Radioactivity (ng-eq/ml)
Traxoprodil (ng/ml)
Concentration (ng or ng-eq/ml)
Time (h)
10000
1000
100
10
1
0.1
0
2
4
6
8
10
12

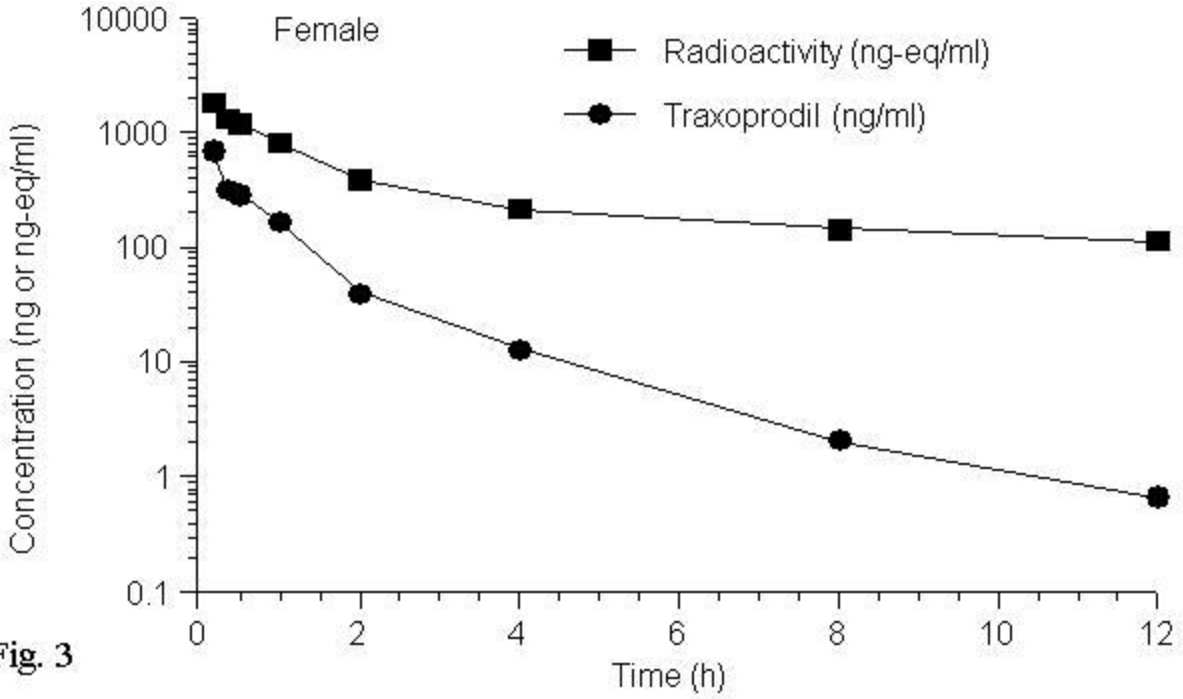
Female
Radioactivity (ng-eq/ml)
Traxoprodil (ng/ml)
Concentration (ng or ng-eq/ml)
Time (h)
10000
1000
100
10
1
0.1
0
2
4
6
8
10
12

Fig. 3

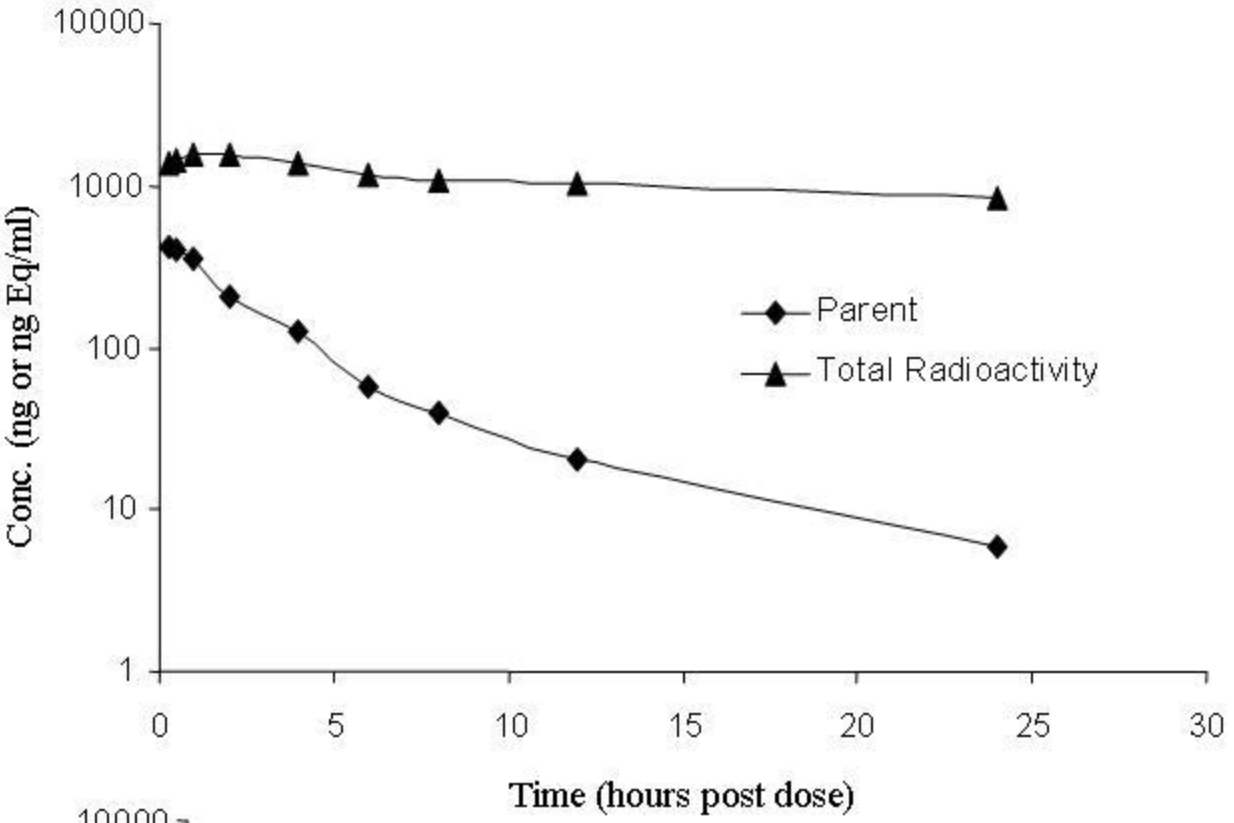
10000
1000
100
10
1
Conc. (ng or ng Eq/ml)
Parent
Total Radioactivity
0
5
10
15
20
25
30
Time (hours post dose)

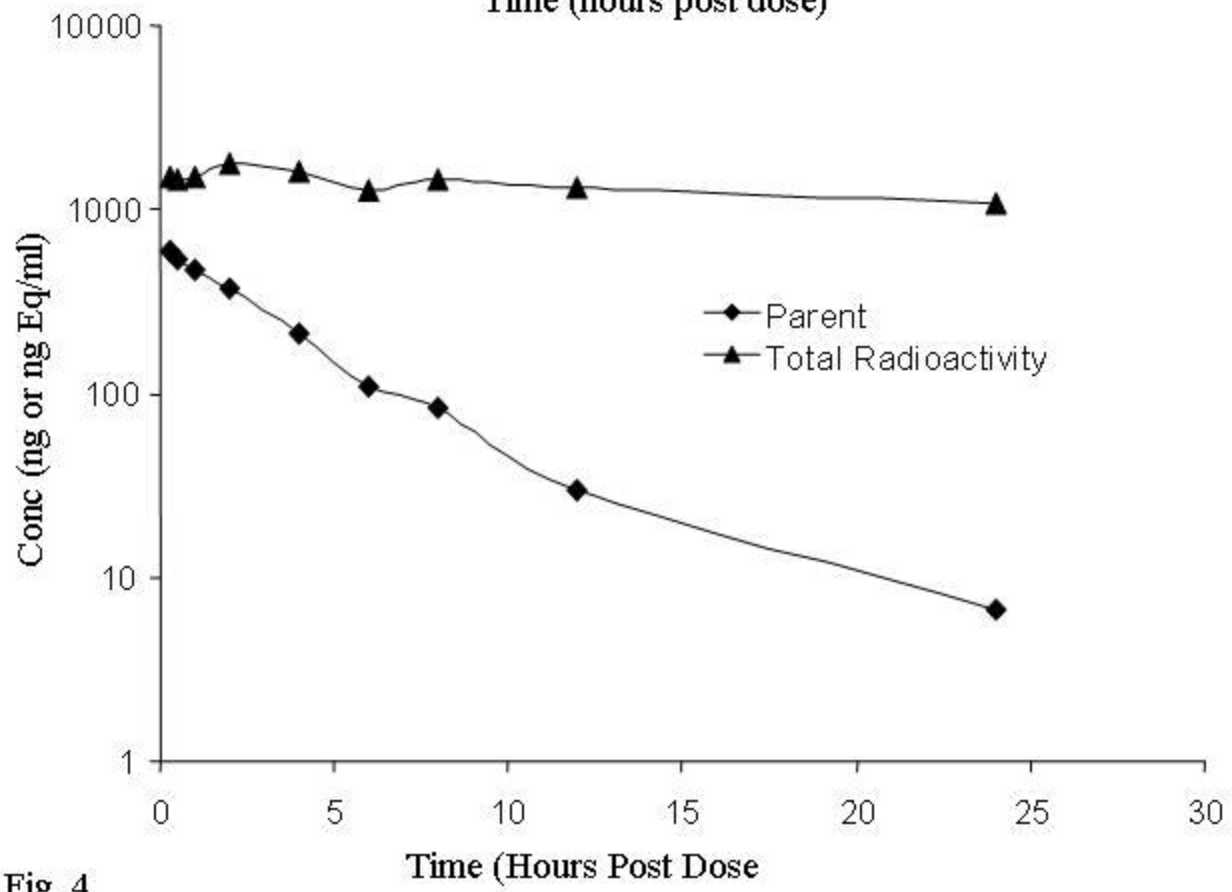
10000
1000
100
10
1
Conc (ng or ng Eq/ml)
Parent
Total Radioactivity
0
5
10
15
20
25
30
Time (Hours Post Dose

Fig. 4

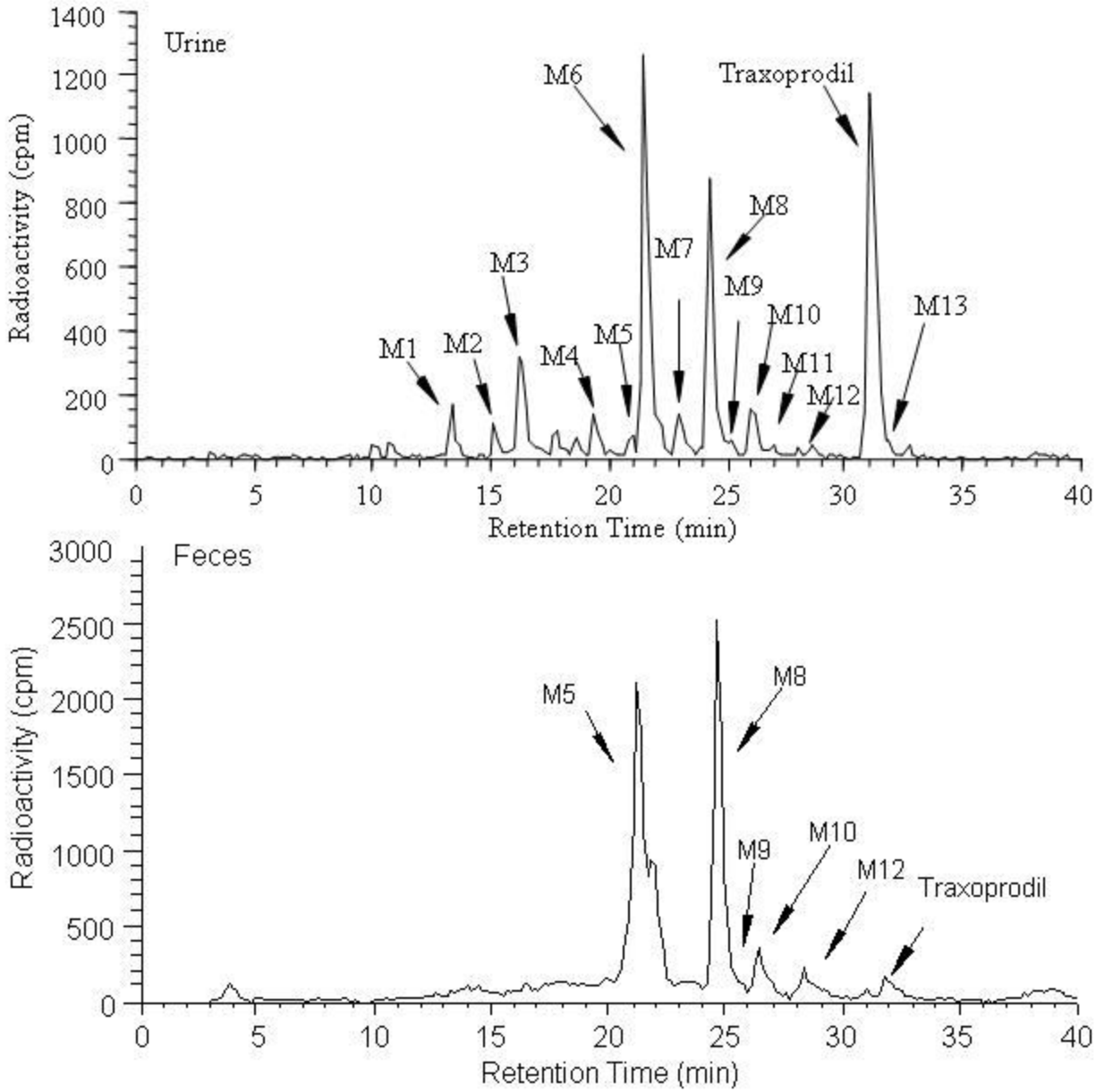

Fig. 5

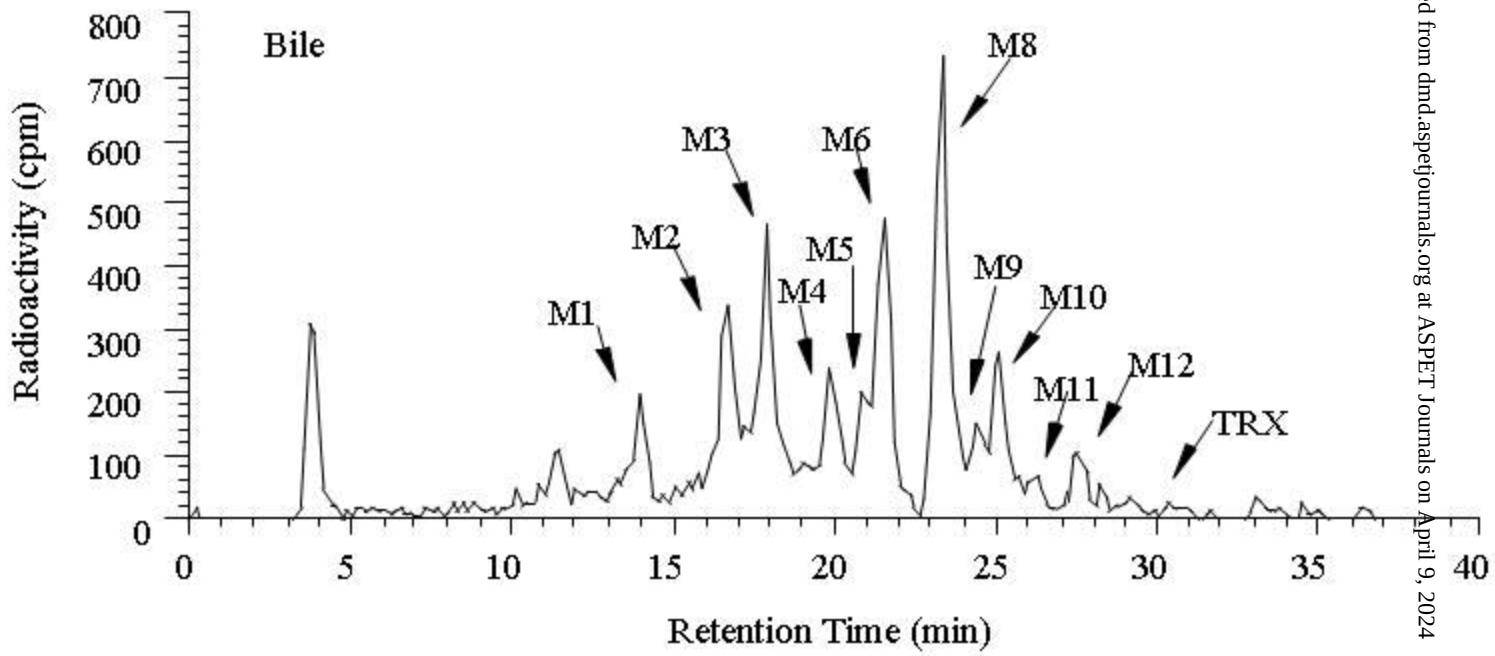

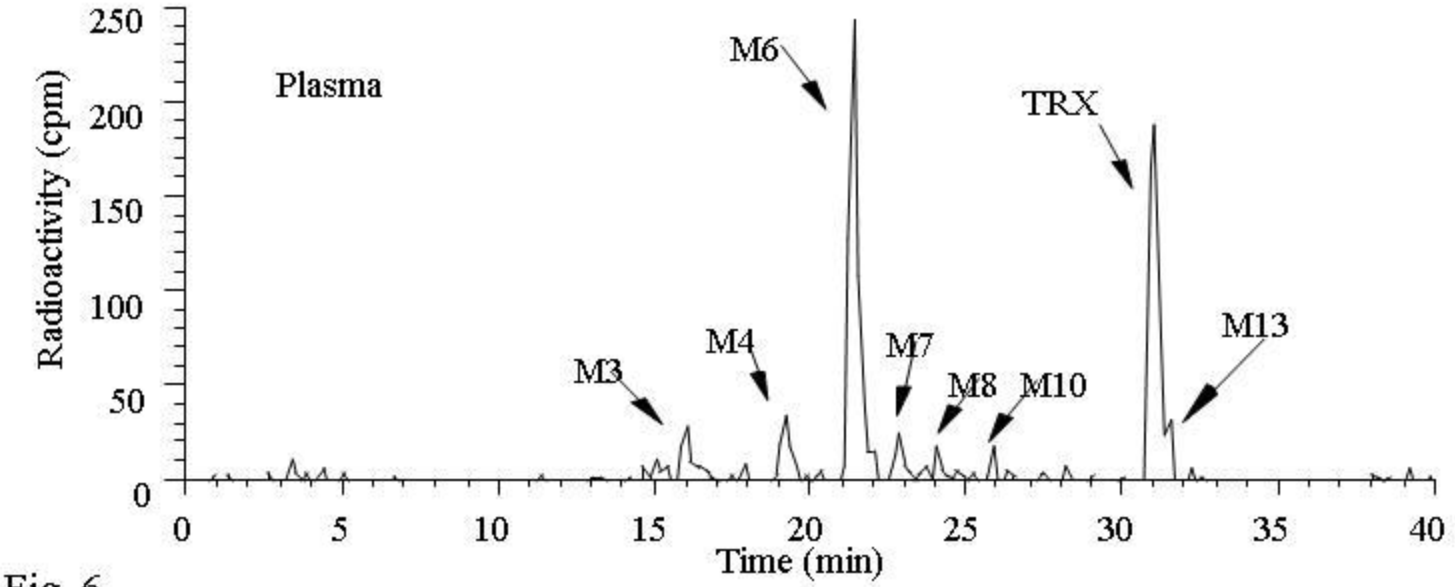

Fig. 6

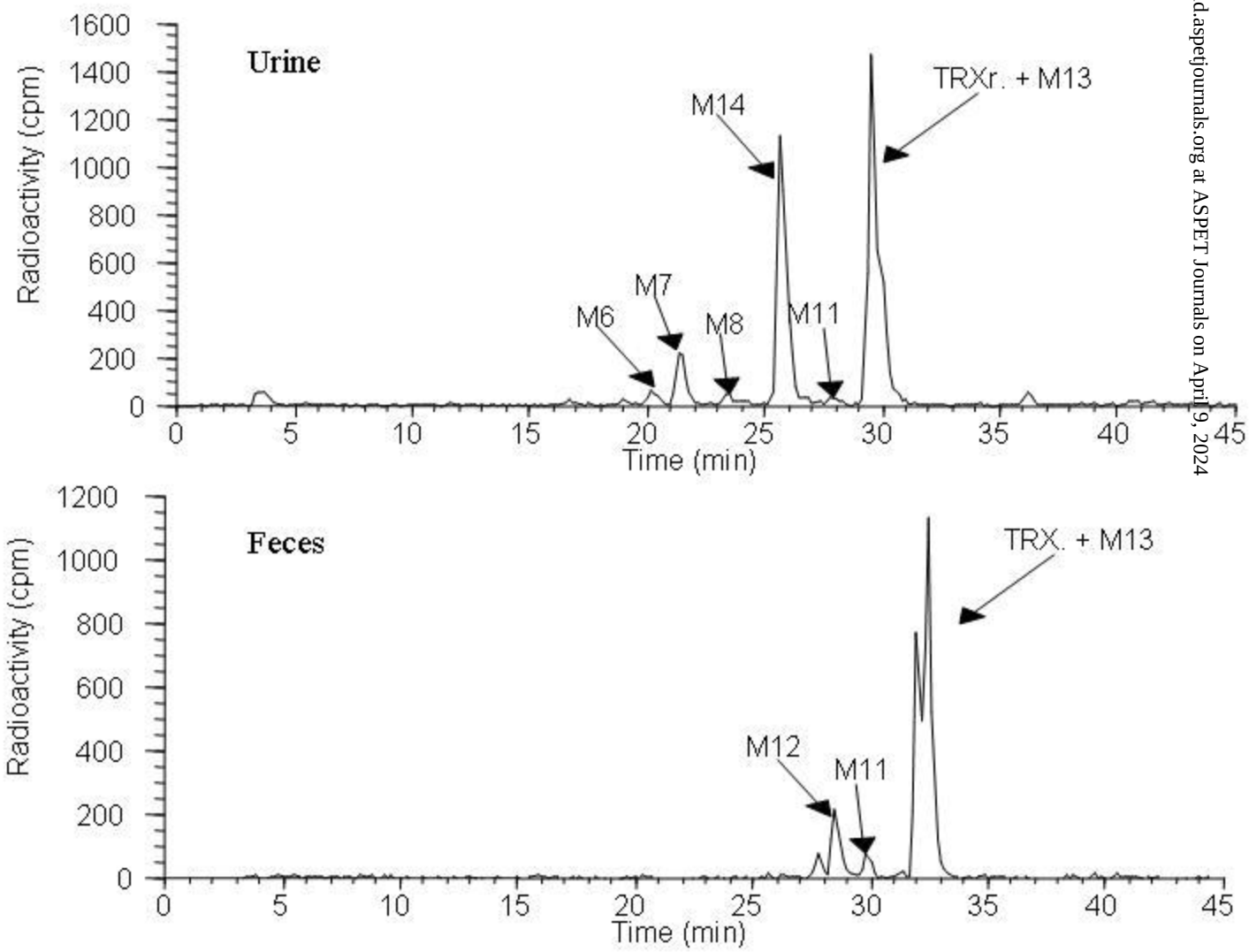

Fig. 7

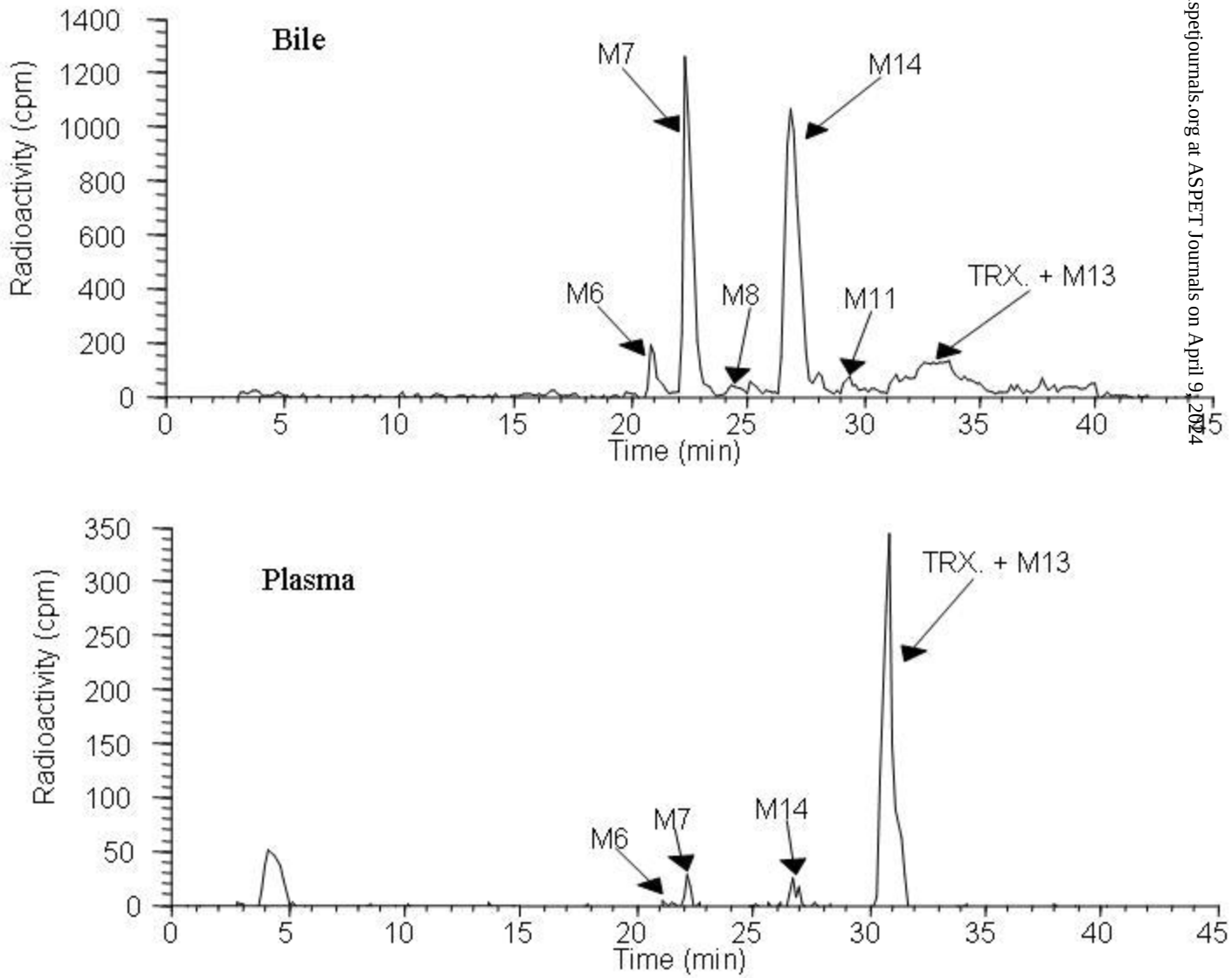

Fig 8

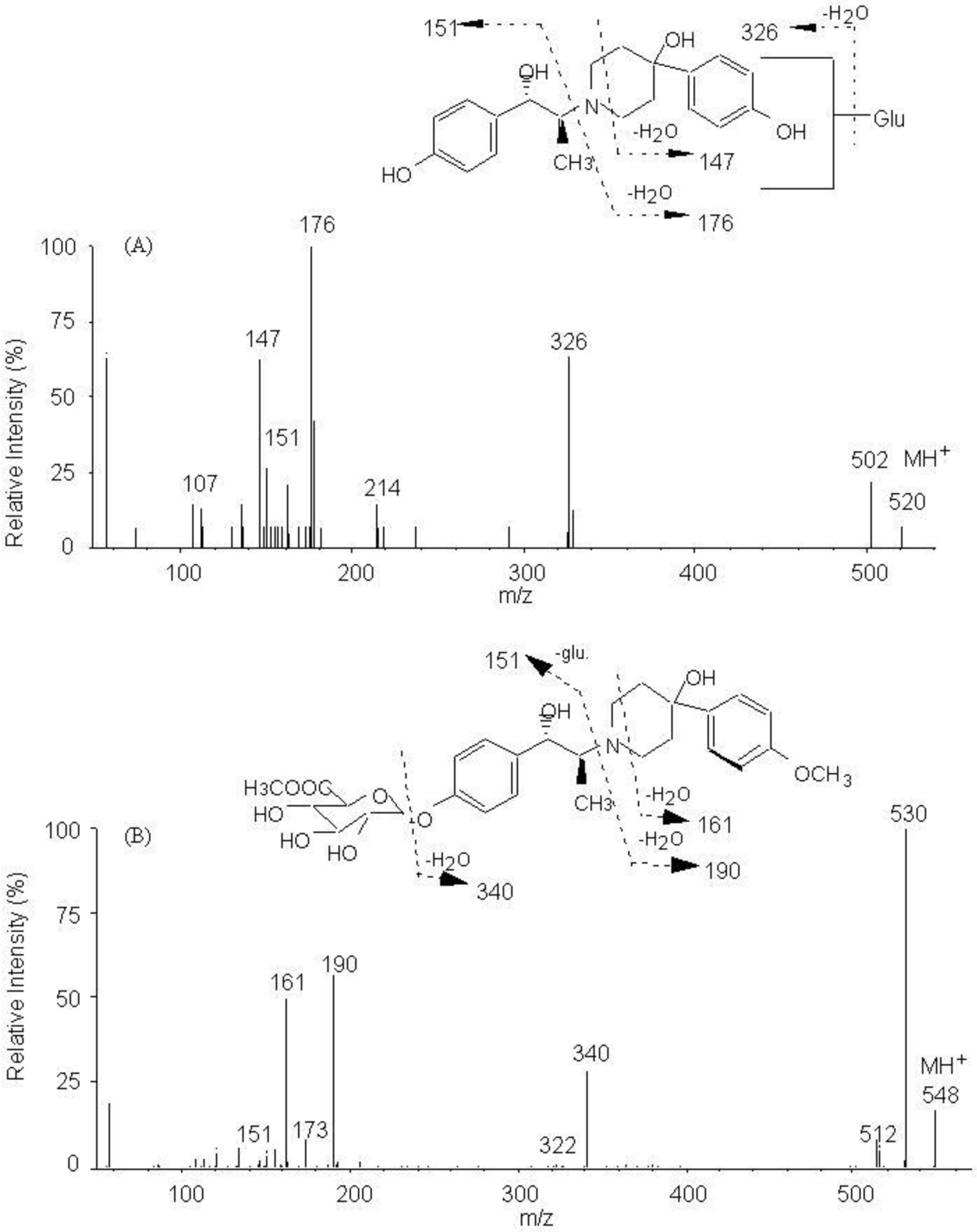
151
326
-H2O
OH
OH
N
Glu
OH
-H2O
147
HO
CH3
-H2O
176
176
(A)
100
75
50
25
0
Relative Intensity (%)
147
326
151
107
214
502
MH+
520
100
200
300
400
500
m/z
151
-glu.
OH
OH
N
OCH3
H3COOC
HO
HO
HO
O
O
CH3
-H2O
161
-H2O
190
-H2O
340
530
(B)
100
75
50
25
0
Relative Intensity (%)
161
190
340
MH+
548
151
173
322
512
100
200
300
400
500
m/z

Fig. 9

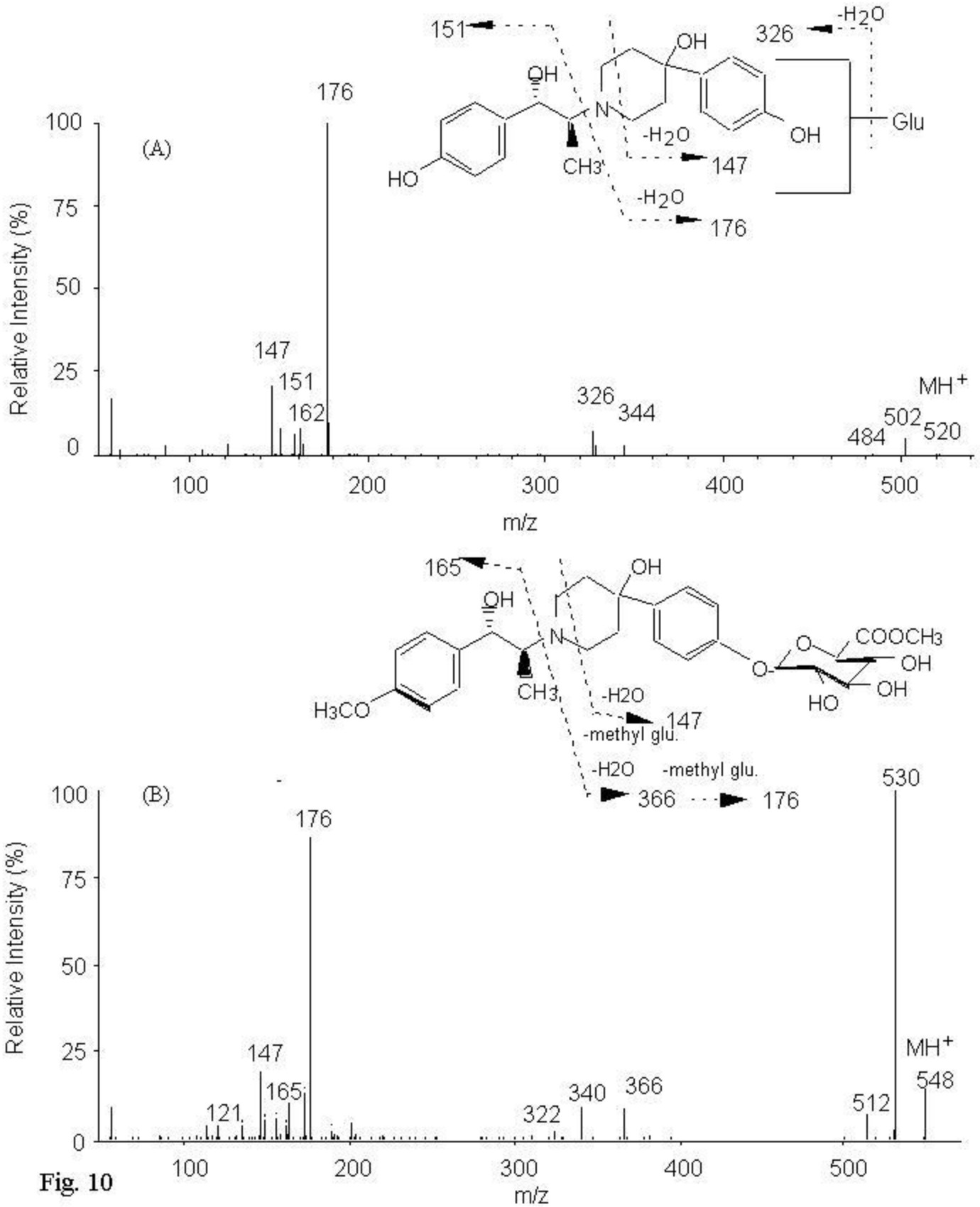
(A)
Relative Intensity (%)
m/z
176
147
151
162
326
344
484
502
520
MH+
151
326
-H2O
OH
OH
N
Glu
OH
HO
CH3
-H2O
147
-H2O
176
(B)
Relative Intensity (%)
m/z
176
147
165
121
322
340
366
512
530
MH+
548
165
OH
OH
N
CH3
H3CO
-H2O
147
-methyl glu.
-H2O
-methyl glu.
366
176
O
COOCH3
OH
OH
HO

Fig. 10